# The effect of turbulence on fog formation

By BERTIL RODHE, *Swedish Meteorological and Hydrological Institute, Stockholm*

(Manuscript received November 21, 1961)

ABSTRACT

Of prevalent conceptions of the physics of fog formation, the "classical" theory of the mixing of air masses of different temperatures seems to the present author to be the most convincing. In view of the fact that turbulent exchange implies a mixing of eddies of different origins, it is clear that the theory of turbulence applied to saturated air should result in some basic ideas of fog formation. For simplification of the problem to be studied, the author assumes that the inertia of the drops of fog can be neglected and that they are transferred by eddies in the same way as vapour. On that assumption, the mixing ratio of the total water content, i.e. the mixing ratio of liquid water plus vapour, and the potential wet-bulb temperature are two elements of air that remain constant in eddies irrespective of whether these are saturated or unsaturated by vapour. By putting each of the elements into the differential equation of eddy exchange, the basic formulae for estimation of fog density are obtained. The boundary conditions of integration determine the alternative kinds of fog, for example advection fog and radiation fog. Finally, some important modifications are obtained if regard is paid to the black-body emissivity of the drops of the fog. Thus, the density of the fog is considerably increased by a rise of the level of radiative heat loss from the ground surface to the top of the fog.

## Contents

1. Introduction
2. The effect of the convective heat loss
3. The effect of the radiative heat loss
4. The effect of the mixing of damp air masses
5. The thermodynamics of saturated air
6. The thermodynamics of unsaturated air
7. The eddy transfer of heat content and water content
8. The distribution of liquid-water content in a temperature transition layer
9. The formation of advection fog
10. The formation of radiation fog
11. The effect of the black-body emissivity of drops on radiation fog
12. The effect of the selective emissivity of vapour and carbon dioxide
13. The effect of the black-body emissivity of drops on advection fog
14. Conclusions

Appendixes.

A. List of symbols
B. The integration of $Y_{\frac{1}{2}}(\alpha,1)$

## 1. Introduction

Fog and cloud formation are the result of the co-action of two different kinds of physical operations. The more obvious of these is the process of transformation of water from the gaseous to the liquid state. It is brought about by small particles of substances that act as nuclei on which liquid water condenses. The nuclei of condensation are so abundant in the atmosphere that in what follows we may presuppose that vapour pressure does not exceed saturation pressure.

The other physical operation which is needed is some kind of atmospheric activity by means of which saturation and a perceptible concentration of liquid water are brought about. The drop density in fog and clouds is about 0.1 g $m^{-3}$ or more (NYBERG, 1949). Owing to the decrease of saturation vapour pressure with temperature, unsaturated air is most effectively transformed into the state of saturation by cooling. Only a slight degree of cooling is needed in order to change the relative humidity considerably.

One cause of cooling is that of adiabatic decrease of pressure. It is combined with convective rise of air and with upslope wind motion and is the essential cause of cloud formation. But adiabatic cooling does not play any significant role in fog formation, since the pres-

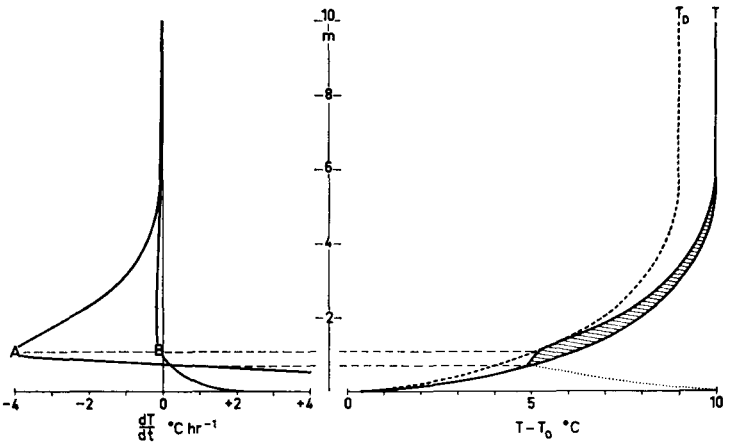


FIG. 1. *Right:* Vertical temperature distribution computed from the equation (1) using $\gamma = 9.0\ 10^{-3}\text{cm}^{-1}$ and $T_a - T_0 = 10°\text{C}$. $T_D$ = the dew-point distribution. *Left:* Vertical distribution of rate of radiative temperature change, computed for a temperature profile of the form given on the right, using (*A*) $\gamma = 9.0\ 10^{-3}\text{cm}^{-1}$, (*B*) $\gamma = 1.6\ 10^{-3}\ \text{cm}^{-1}$. *Right:* The shaded area and the dotted line below 70 cm represent the 15-minute radiative temperature change according to (*A*). Reproduced from FLEAGLE (1953).

sure changes next to the ground are too slow. The air of the surface boundary layer is either cooled by advection over a cold surface or by radiative heat loss at the surface. It seems to the present author that in each of the two cases the essential cause of fog formation is the turbulent mixing which is combined with the eddy transfer of heat content and water content between the level of unmodified air at the top of the boundary layer and the ground surface at the base. It follows from this hypothesis that a warm, wet surface should have the same effect as a cold one. Indeed, that alternative is encountered in the formation of "sea smoke" or "steam fog".

## 2. The effect of the convective heat loss

Simultaneously with the eddy transfer of heat content, there is an eddy exchange of vapour content. Between a warm, almost saturated air layer and a cold ground surface, the net transfer of the heat content and that of the vapour are both directed downwards. At the ground, moisture is deposited as dew. Mathematically, the process of eddy transfer of vapour is expressed by the same kind of differential equation as the eddy heat transfer. The coefficient of eddy exchange of vapour does not greatly differ from that of eddy heat transfer. In consequence, a cooling effect runs simultaneously with an effect of "drying" and, in spite of cooling, the air does not always become saturated.

The ability of eddy exchange to bring about saturation by heat loss was first questioned by G. I. TAYLOR (1917), later by EMMONS & MONTGOMMERY (1947). By means of some diagrams, Taylor showed that in fact there is a decrease of moisture in the air above a surface which is cooled by radiative heat loss. He put forward the theory that the formation of fog next to a cold surface is not the direct consequence of cooling but is rather an effect of turbulent mixing. Indeed, he brought up the idea that lies behind the present paper, but he did not develop it mathematically as will be done in what follows.

In their note of 1947, EMMONS & MONTGOMMERY also made the above-mentioned statement, but they followed another theoretical line and pointed out the effect of cooling by the radiative emissivity of the air itself. Their idea will be discussed in the next section with reference to a paper of FLEAGLE (1953).

## 3. The effect of the radiative heat loss

As mentioned above, EMMONS & MONTGOMMERY advanced the theory that the radiation

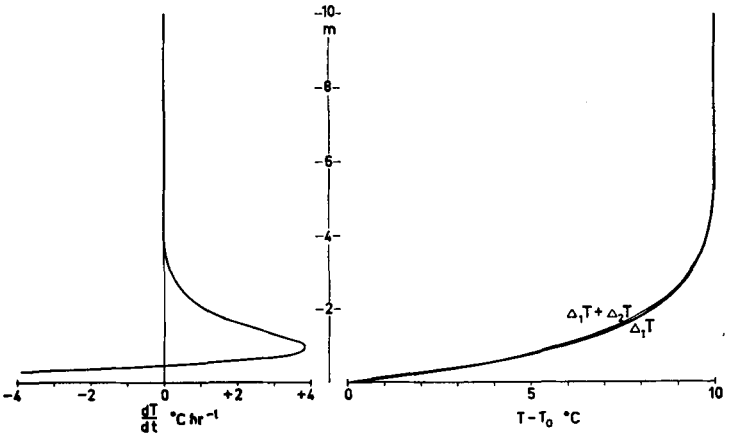


FIG. 2. The effect of a change of the vertical temperature profile on the eddy exchange of heat content. The thick profile curve ($\Delta_1 T$) on the right is assumed to be related to a steady state without any loss or gain of heat within the air layer. The thin curve ($\Delta_1 T + \Delta_2 T$) includes a slight change of the profile that is great enough to bring about the great heating and cooling effects shown on the left.

of the air itself might be an effect that brings about cooling and fog formation. Inspired by this idea, FLEAGLE (1953) made a quantitative estimation. The diagram by means of which he illustrates his computation is reproduced in Fig. 1.

The existence of a ground surface is necessary for the persistence of the temperature profile shown in the right-hand part of the figure. Heat balance is there established partly by a net downward eddy transfer of heat, partly by a net upward radiative flux of heat. The radiative heat loss at the ground surface is due to the black-body emissivity of the surface, which radiates also in the transparent part of the spectrum of moist air. In the other part of the spectrum, the molecules of vapour and carbon dioxide absorb and emit long-wave radiation, and a net flux of radiation is established between parts of different temperature within the surface boundary layer. In the lower part of the inversion layer of Fig. 1 the air is heated, since it does not emit as much as it absorbs of the radiation from the warmer upper part. In the upper part, however, the air is cooled, owing to the radiative outflow that dominates there in consequence of the higher temperature of the upper part in relation to the lower. In his diagram Fleagle has chosen a temperature difference of 10°C between the surface and the upper, unmodified air. The temperature profile in the intermediate transition layer is put by him in the form

$$T - T_0 = (T_a - T_0)(1 - e^{-\gamma z}), \qquad (1)$$

where $T_a$ is the temperature of the upper, unmodified air and $T_0$ that of the surface.

In the left-hand part of the figure, the distribution of the radiational change of temperature is shown. The curve marked $A$ refers to the temperature profile represented by $\gamma = 9.0\ 10^{-3}$ cm$^{-1}$ and shown on the right. The curve marked $B$ is based on $\gamma = 1.6\ 10^{-3}$ cm$^{-1}$ and is related to a temperature gradient that in the lowest part of the transition layer is slightly less than that shown in the figure.

As shown, the maximum rate of temperature change is the greater the steeper is the temperature gradient in the lowest part of the transition layer. The gradient has little effect on the height of the level that separates the cooling layer from the heating layer. Fleagle estimated the height at about 70 cm.

By means of a shaded area and a dotted line in the figure, Fleagle illustrated the temperature profile that will result in consequence of the above-mentioned radiation during 15 minutes. Fleagle concluded that his estimation supported the hypothesis of Emmons & Montgommery as regards the effect of the emissivity of the air itself in bringing about fog formation.

However, Fleagle disregarded the additional effect of eddy exchange that tends to diffuse sinks and sources of heat. In the subsequent part of the present section it will be shown that even a much smaller change of the tempera-

ture profile than that sketched by Fleagle induces an eddy heat exchange that is capable of balancing the radiative effect.

We divide the temperature profile into two parts,

$$T - T_0 = \Delta_1 T + \Delta_2 T. \tag{2}$$

The first part is identical with the primary profile represented by (1) and shown in Fig. 1,

$$\Delta_1 T = \Delta_1 T_a (1 - e^{-\gamma z}). \tag{3}$$

It is assumed to maintain a constant heat transfer,

$$\frac{\partial}{\partial z}\left[K_H \frac{\partial \Delta_1 T}{\partial z}\right] = 0. \tag{4}$$

This means that the coefficient of eddy exchange varies according to

$$K_H = K_0 e^{\gamma z}. \tag{5}$$

The second part of (2) represents the change of the temperature profile induced by radiation as described by Fleagle. For simplicity, we put it in a sine form, for example,

$$\Delta_2 T = \Delta_2 T_a \sin [\tfrac{3}{2}\pi e^{-\gamma z}]. \tag{6}$$

Below $z = 0.41\gamma^{-1}$, where $e^{-\gamma z} = \frac{2}{3}$, the sign of $\Delta_2 T$ is opposite to that of $\Delta_2 T_a$. Above that level, $\Delta_2 T$ and $\Delta_2 T_a$ have the same sign. A negative sign of $\Delta_2 T_a$ relates to the effect of radiation sketched by Fleagle in Fig. 1.

In the first instance, we assume that the coefficient of eddy exchange still varies in accordance with (5). Because of that, the eddy transfer of heat is not constant along the vertical when the temperature profile departs from (3). As regards the profile of (2), we get

$$\frac{dT}{dt} = \frac{\partial}{\partial z}\left[K_H \frac{\partial \Delta_2 T}{\partial z}\right]. \tag{7}$$

In terms of (5) and (6), (7) reads

$$\frac{dT}{dt} = -\frac{9}{4}\gamma^2 \pi^2 K_0 \Delta_2 T_a e^{-\gamma z} \sin\left[\frac{3}{2}\pi e^{-\gamma z}\right]. \tag{8}$$

We put $\gamma = 9.0\ 10^{-3}$ cm$^{-1}$ as in Fig. 1, $K_0 = 10$ cm$^2$ sec$^{-1}$ and $\Delta_2 T_a = -0.15$°C. The temperature distribution that is related to these constants is shown in the right-hand part of Fig. 2, which is drawn on the same scale as Fig. 1. The temperature change that results from turbulence is found in the left-hand part. We see that it is almost a mirror image of the left-hand part of Fig. 1. The temperature profile that induces this image, however, differs hardly perceptibly from the primary profile. The difference will not be measurable at atmospheric conditions by means of ordinary thermometric methods.

Some years later, Fleagle (1956) showed that measurements of refractive differences in the temperature transition layer next to a cold water surface indicated an anomaly of the temperature gradient at about 10 cm above the surface. This anomaly might be an effect of the radiation of the air itself as described above. By numerical integration of the data, Fleagle constructed the temperature profile. The magnitude of the anomaly of temperature at about 10 cm above the surface was about the same as that in Fig. 2.

We conclude that the sinks and sources of radiative heat exchange are easily balanced by eddy transfer of heat even in the case of very small temperature anomalies induced by radiation. In Fig. 2, the magnitude of the vertical variation of eddy heat transfer is, in terms of the unmodified transfer,

$$\frac{-K_H \dfrac{\partial \Delta_2 T}{\partial z}}{-K_H \dfrac{\partial \Delta_1 T}{\partial z}} = -\frac{3}{2}\pi \frac{\Delta_2 T_a}{\Delta_1 T_a} \cos\left[\frac{3}{2}\pi e^{-\gamma z}\right].$$

With the values attributed to $\Delta_1 T_a$ and $\Delta_2 T_a$ above, we find that the magnitude does not exceed 7%. Robinson (1950) and Rider & Robinson (1951), who measured the eddy heat transfer, the radiative heat flux and the corresponding vertical variations in clear air above short grass, found in the lowest metre relative variations that were up to 10%. Thus, our illustration of the problem does not seem to be unrealistic.

Furthermore, the investigation of Rider & Robinson supports the theory that the temperature variations in the air layer are the result of co-action of convective heat loss (or gain) and radiative heat gain (or loss). In most cases the difference between the two concepts is small (less than one per cent of the eddy heat transfer), but is sufficiently large to bring about temperature fluctuations.

Another view of the problem is given by LILJEQUIST (1957). He studied the energy balance at the snow surface in the very extreme conditions found in the Antarctic. He found that in very strong, well-developed inversions (i.e. cases of almost linear, vertical increase of temperature established by radiative net outflow), the eddy transfer of heat is independent of the temperature gradient because the coefficient of eddy exchange is in inverse proportion to the temperature gradient. This implies that it was not quite correct in our procedure to put the coefficient constant regardless of variations of the temperature gradient.

Liljequist's conclusion is based on average conditions of a boundary layer, 10 metres deep, above the snow surface. Hence, it is not certain that the correlation between the gradient and the coefficient holds good in temporary vertical variations. The profiles that Liljequist illustrates have numerous types of discontinuities of gradient. The simple form of the profiles of Figs. 1 and 2 is related by him to young, undeveloped inversions. At low wind speeds and net outgoing radiation, it is soon transformed into a straight profile with one or two, or even more, discontinuities of gradient. In Fig. 3 there are reproduced six types of such "mature" inversion profiles. It seems possible that the transformation into the "mature" form may be due to radiative cooling as described by Fleagle. In such a case, discontinuities of eddy heat transfer are established along the vertical in order to balance the sinks and sources of radiation. But the discontinuities found in the temperature profiles are often so great that the radiative effect would be far exceeded by the effect of turbulence if there were not a negative correlation between the gradient and the coefficient of eddy exchange. When such a correlation exists, a great discontinuity of the temperature gradient may be coupled with a relatively small change of eddy heat transfer that exactly balances the small radiative effect of the air.

To sum up, then, we can say that in certain conditions the long-wave emissivity of vapour and carbon dioxide may bring about perceptible cooling of the air in a surface boundary layer. But we maintain that the cooling is an effect of combined action of radiative heat exchange and eddy heat transfer. That is why we maintain that the process of fog formation cannot be seen as a direct effect of radiative cooling only. In what follows we shall discuss the process, taking into consideration the concepts of eddy transfer, but at first disregarding the long-wave emissivity of moist air. Later, in Section 12, we shall re-examine that factor in the light of the discussion in the sections which now follow.

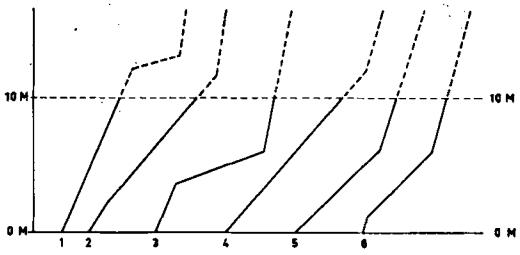


FIG. 3. Diagrammatic presentation of "mature" inversions in the surface layer next to an Antarctic snowfield. Reproduced from LILJEQUIST (1957).

## 4. The effect of the mixing of damp air masses

In addition to the effect of cooling, mixing of two air masses of different temperatures is pointed out in textbooks of meteorology as a cause of fog formation. The theory is an old one. In the nineteenth century it bore the name of James Hutton (1726–97) and implied that the mixing effect was the cause of precipitation. However, the amount of perceptible water was overestimated, since no regard was paid to the effect of heating by the release of latent heat. This was probably first pointed out by WETTSTEIN (1869). But Wettstein overestimated the effect of heat release and concluded that mixing might not bring about any condensation at all! HANN (1874) gave a correct view; he showed that the amount of liquid water produced was considerable but too small to bring about moderate precipitation. He realized that the adiabatic cooling of rising air is the principal cause of saturation in the formation of clouds. In 1882 PERNTER presented a first mathematical deduction of the mixing effect. In a paper of 1890 VON BEZOLD dealt exhaustively with the topic. In a series of diagrams, he gave graphical representations of the relation between the original air masses and the final mixture.

When TAYLOR in 1917 reviewed the problem of fog formation in the light of empirical data,

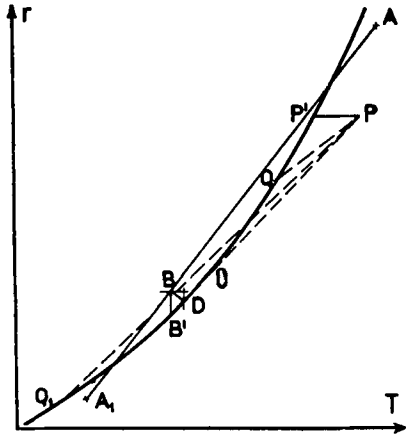


FIG. 4. $T,r$ diagram illustrating the effect of the mixing of damp air masses with reference to VON BEZOLD (1890), TAYLOR (1917) and BRUNT (1935).

he made the same mistake as Hutton and neglected the heat released by condensation. Attention was drawn to this by BRUNT (1935) in a short note. Brunt agreed with Hann and von Bezold as regards the magnitude of liquid water in the mixture and concluded (1944) that "the formation of fog at a surface of discontinuity in the atmosphere is to be explained, at least in part, by the effect of mixing of masses of air of different temperatures and humidities".

The fundamental physical reason why mixing results in saturation is found in the curvature of the line that represents the saturation-vapour mixing ratio as a function of temperature. In the diagram in Fig. 4, the state of air is represented by a point of which the abscissa is the temperature and the ordinate corresponds to the water mixing ratio. The curve of saturation-vapour mixing ratio divides the diagram into two parts. To the left of the curve, the air is saturated by vapour; to the right, it is unsaturated. When two air masses that differ in temperature (points $A$ and $A_1$ in the diagram) are mixed, there may result a vapour mixing ratio that is greater (at $B$) than that of saturation (at $B'$) at the temperature of the mixture. But owing to the release of latent heat by condensation, the final temperature is not that of $B$ but that of $D$. In consequence, the excess of mixing ratio is not equivalent to $BB'$ but to the projection of $BD$ along the ordinate.

As mentioned above, Taylor found that the cooling effect of convection was not capable of bringing about saturation and he tried to find the explanation of fog formation above a cold surface in the following way. In the diagram reproduced in Fig. 4, he assumed the unmodified and unsaturated air above the surface to be represented by a point $P$ and the wet, cold surface by a point $Q$. Since the conditions in the transition layer between $P$ and $Q$ are brought about by mixing of saturated air originating at $Q$ and unsaturated air originating at $P$, the temperature and the humidity at intermediate levels are found along the line $PQ$. From $P$, Taylor drew a tangent that touched the saturation curve at $O$. He concluded that the condition for fog formation in the transition layer was that the temperature of the surface (for example that at the point $Q_1$) should be below that at $O$. In such a case, the curve $PQ_1$ of the relation between temperature and humidity partly runs to the left of the saturation curve.

Taylor's discussion is very interesting. It combines the "classical" idea of the effect of mixing with the theory of eddy exchange. Turbulence implies mixing of eddies and, in the transition layer next to a cold surface, eddies that descend from the unmodified air are mixed with others that are strongly modified by the surface. At each level in the transition layer, the temperature as well as the humidity is determined by the proportions of eddies brought together by turbulence from different levels. Accordingly, the problem of the distribution of liquid water in fog involves the question how to apply the methods of theory of eddy exchange to saturated air.

In the next two sections, the thermodynamics of saturated air will be studied in order to find characteristic elements that remain constant in closed eddies moving upwards and downwards, irrespective of whether the eddies are saturated by vapour or not. We shall assume that the liquid drops which are condensed in the eddies are so small that their inertia against eddy changes of velocity is negligible. On this condition, we shall find that the wet-bulb potential temperature and the mixing ratio of the total water content have the property claimed.

## 5. The thermodynamics of saturated air

The *First Law of Thermodynamics* gives the amount of heat $q_1$ that should be added to

a system of dry air or be taken away from it in order to bring about the changes $dT$ of its temperature and $dp$ of its pressure,

$$q_1 = c_p\,dT - \frac{1}{\varrho}dp, \tag{9}$$

where $c_p$ is the specific heat of dry air at constant pressure, $\varrho$ the density of dry air at temperature $T$ and pressure $p$. In a system of vapour that is in equilibrium with suspended liquid drops, the law reads

$$q_2 = (cw + c'v)dT + L\,dv, \tag{10}$$

where $c$ is the specific heat of water, $c'$ that of saturated vapour, $L$ the latent heat of evaporation at temperature $T$. The effect of drop surface curvature as well as that of salt content on vapour pressure are disregarded. The total content of vapour and drops in the system is constant if the system is closed and neither receives nor loses any drops or vapour. We specify the content by means of the mixing ratio ($r$) which expresses the relative proportions by weight of water and dry air in a given volume of saturated air. The mixing ratio of the total water content is the sum of the corresponding concepts of vapour ($v$) and liquid water ($w$),

$$r = v + w. \tag{11}$$

Provided that the heat amount is added or taken away by means of a reversible process, the change of entropy S in a system of dry air is

$$d\mathrm{S}_1 = c_p dT/T - R\,dp/p \tag{12}$$

and in a system of vapour and water drops

$$d\mathrm{S}_2 = (cw + c'v)dT/T + L\,dv/T, \tag{13}$$

$R$ being the gas constant for dry air. The theory of thermodynamics states that the differential of entropy is an exact one. In the case of dry air (12) this is immediately clear, since $c_p$ and $R$ are constants. In the case of the system of vapour and drops (13), the statement implies that

$$\frac{c\left(\frac{\partial w}{\partial v}\right)_T + c'}{T} = \left[\frac{\partial\left(\frac{L}{T}\right)}{\partial T}\right]_v. \tag{14}$$

In a closed system, the water content $r$ in equation (11) is constant, and the derivative in the left-hand member is equal to $-1$. In consequence, (14) reads

$$c' = c + T\left(\frac{\partial(L/T)}{\partial T}\right)_v, \tag{15}$$

and (10) assumes the form

$$q_2 = \left[cr + T\frac{d(Lv/T)}{dT}\right]dT. \tag{16}$$

Adding (9) and (16), we get the change of heat of a system of saturated air plus water drops,

$$q_1 + q_2 = \left[c_p + cr + T\frac{d}{dT}\left(\frac{Lv}{T}\right)\right]dT - RT\frac{dp}{p}. \tag{17}$$

We assume that the total system of air, vapour and drops is closed. This means, first, that $r$ in (11) is constant. Secondly,

$$q_1 + q_2 = 0. \tag{18}$$

In consequence, a potential temperature $\theta$ that we define by means of the formula

$$\left[c_p + cr + \theta\frac{d}{d\theta}\left(\frac{Lv}{\theta}\right)\right]_p \frac{d\theta}{\theta} = \left[c_p + cr + T\frac{d}{dT}\left(\frac{Lv}{T}\right)\right]\frac{dT}{T} - R\frac{dp}{p} \tag{19}$$

remains constant in a closed system at pressure variations.

## 6. The thermodynamics of unsaturated air

In unsaturated air, the wet-bulb temperature $T'$ is theoretically related to the temperature $T$ of the dry bulb by means of the formula

$$(c_p + c_p' r)(T - T') = L(v' - r). \tag{20}$$

The formula is based on the process of evaporation that takes place on the wet bulb of a psychrometer. The latent heat required for saturation (right-hand member) is released by cooling of the air (left-hand member). $c_p'$ is the specific heat of unsaturated vapour. By adding equal

terms to each member, we get *Normand's Proposition I*,

$$c_p T + crT' + Lr + c_p' r(T - T') = c_p T' + cv'T' + Lv' - c(v' - r)T'. \quad (21)$$

In the words of BRUNT (1944) the proposition reads: "The heat content of the air is equal to the heat content of the same air saturated at the wet-bulb temperature, *minus* the heat content of the additional liquid water required so to saturate it."

It is easy to find that the right-hand member of the equation is identical with

$$(c_p + cr)T' + Lv'. \quad (22)$$

In consequence, (22) is the heat content of unsaturated air in terms of the wet-bulb temperature. We recall that $v'$ is the saturation mixing ratio at the temperature of the wet bulb.

In the psychrometric process, heat is released by the air at a higher temperature than that at which it is used for evaporation on the wet bulb. That is why the psychrometric process of evaporation is not a reversible one. However, *Normand's Proposition II* gives an idea of the thermodynamic balance that would prevail in the case of a hypothetically reversible psychrometric process. The proposition reads in the words of BRUNT (1944): "The entropy of air is equal to the entropy of the same air saturated at the wet-bulb temperature, *minus* the entropy of the additional liquid water required so to saturate it."

Mathematically, the last proposition reads, in conformity with (21),

$$c_p \log \frac{T}{T_0} + cr \log \frac{T'}{T_0} + \frac{Lr}{T'} + c_p' r \log \frac{T}{T'} = c_p \log \frac{T'}{T_0} + cv' \log \frac{T'}{T_0} + \frac{Lv'}{T'} - c(v' - r) \log \frac{T'}{T_0}. \quad (23)$$

The temperature $T_0$ is an arbitrary point of reference. The right-hand member is easily found to read

$$(c_p + cr) \log \frac{T'}{T_0} + \frac{Lv'}{T'}. \quad (24)$$

Thus, (24) is the entropy of unsaturated air in terms of the wet-bulb temperature.

The thermodynamic definition of specific heat at constant pressure is either

$$\left(\frac{\partial \mathbf{H}}{\partial T}\right)_p \quad \text{or} \quad T\left(\frac{\partial \mathbf{S}}{\partial T}\right)_p, \quad (25)$$

where **H** is the heat content and **S** the entropy of one unit of mass.

By application of (25) to (22) and (24), we get

$$\left[c_p + cr + \frac{d}{dT'}(Lv')\right]\frac{dT'}{dT} \quad (p \text{ const}) \quad (26)$$

and

$$\left[c_p + cr + T'\frac{d}{dT'}\left(\frac{Lv'}{T'}\right)\right]\frac{T}{T'}\frac{dT'}{dT} \quad (p \text{ const}) \quad (27)$$

respectively. The specific heat in the form of (26) is not the least possible since it is based on an irreversible process. The minimum amount of specific heat is found in reversible processes and is identical with that represented by (27). The relative difference of the terms of the brackets in (26) and (27) is 0.3 % at $T' = -30°C$, 2.1 % at $T' = 0°C$ and 4.8 % at $T' = +30°C$ and $r = v'$. The complete terms of (26) and (27) differ still less from each other because of the fraction $T/T'$, which slightly exceeds unity. Thus, a significant error is not introduced when (26) is used instead of (27). In the examples that will follow, the wet-bulb temperature is calculated by means of (20). But in theory, it should be based on *Normand's Proposition II*. On that basis, the *First Law of Thermodynamics* reads, for a system of air plus unsaturated vapour,

$$q_1 + q_2 = \left[c_p + cr + T'\frac{d}{dT'}\left(\frac{Lv'}{T'}\right)\right]\frac{T}{T'}\frac{dT'}{dT}dT - RT\frac{dp}{p}. \quad (28)$$

Provided that the system is closed, neither heat nor liquid water or vapour is received or lost, which means that

$$q_1 + q_2 = 0 \quad (29)$$

and

$$r = v' + w = \text{constant}. \quad (30)$$

Here, $-w$ *is the liquid water required to saturate the air* isentropically. It is called the *deficit* of

liquid water. In the case of saturated air discussed in Section 5, we referred $+w$ *to the mixing ratio of drops*, that is the *surplus* of liquid water.

In consequence of (29), the wet-bulb potential temperature $\theta'$, which we define by means of

$$\left[c_p + cr + \theta' \frac{d}{d\theta'}\left(\frac{Lv'}{\theta'}\right)\right]_p \frac{d\theta'}{\theta'} = \left[c_p + cr + T' \frac{d}{dT'}\left(\frac{Lv'}{T'}\right)\right]\frac{dT'}{T'} - R\frac{dp}{p}, \quad (31)$$

remains constant in a closed system which is subject to pressure variations.

Bearing in mind that the wet-bulb temperature does not differ from the dry-bulb temperature in saturated air, we find that the definition of the potential temperature is the same in the cases of saturated air (19) and unsaturated air (31). Even the mixing ratio of total water content is written in the same form in both cases, as is seen in (11) and (30). In what follows, a prime index will be added to the symbols $T$, $\theta$ and $v$ when these refer to saturated air, in order to mark their identity with the corresponding concepts of the wet-bulb temperature of unsaturated air.

## 7. The eddy transfer of heat content and water content

A conservative property of air is diffused by turbulence in the direction of its gradient. In the case of wet-bulb potential temperature, that means an eddy diffusion of total heat content, that is to say sensible-heat content plus latent-heat content,

$$H = -\varrho\left[c_p + cr + \theta' \frac{d}{d\theta'}\left(\frac{Lv'}{\theta'}\right)\right]_p \frac{\theta}{\theta'} \cdot K_H \cdot \frac{\partial \theta'}{\partial z}. \quad (32)$$

The potential dry-bulb temperature $\theta$ is fixed at $\theta'$ by $r$ in the same way as $T$ is related to $T'$ and $r$ in equation (20).

As far as water content is concerned, turbulence results in a transfer of vapour and liquid drops,

$$E = -\varrho K_E \frac{\partial r}{\partial z}. \quad (33)$$

We want to find the relationship between the vertical distributions of $\theta'$ and $r$ at any fixed point $(x, y)$. For that purpose we put $dt$, $dx$ and $dy = 0$ but retain $dz \neq 0$ in the total differentials $d\theta'$ and $dr$ and transform (33) into

$$E = -\varrho K_E \frac{dr}{d\theta'} \frac{\partial \theta'}{\partial z}. \quad (34)$$

By elimination of the temperature gradient, we get the transfer of water content in terms of that of heat content,

$$E = H \cdot \frac{K_E}{K_H} \frac{\frac{\theta'}{\theta}\frac{dr}{d\theta'}}{c_p + cr + \theta' \frac{d}{d\theta'}\left(\frac{Lv'}{\theta'}\right)}. \quad (35)$$

The fraction $E/H$ recalls the *Bowen ratio*—in what follows called $B$—which puts the eddy transfer of sensible heat in relation to that of latent heat (SUTTON, 1953):

$$1 + B = \frac{H}{L \cdot E}. \quad (36)$$

The *Bowen ratio* is used by oceanographers and climatologists for computing the mean evaporation of oceans by means of data on net radiation at the surface. In the present paper, however, it is only used as a concept for the relation between evaporation and convection.

Before entering into further discussion, we make the following assumptions:

(i) $K_H = K_E = K$: By several investigators (e.g. SWINBANK, 1955), differences between various kinds of eddy exchange coefficients have been pointed out. However, any difference that may exist between the coefficient of eddy exchange of vapour and the coefficient of eddy exchange of heat content is not of such a magnitude that it significantly affects the result of the discussion in this paper. If we should object to putting $K_E$ and $K_H$ equal to each other, we might alternatively assume that the fraction $K_E/K_H$ does not vary in the surface boundary layer and retain it as a constant factor in (35).

(ii) $dp = 0$, i.e. $\theta' = T'$: The subject of the following discussion will be the boundary transition layer in the air next to the ground. Cases of steep temperature gradients in that layer will be of special interest. The effect of the pressure term in (31) will be a minor one.

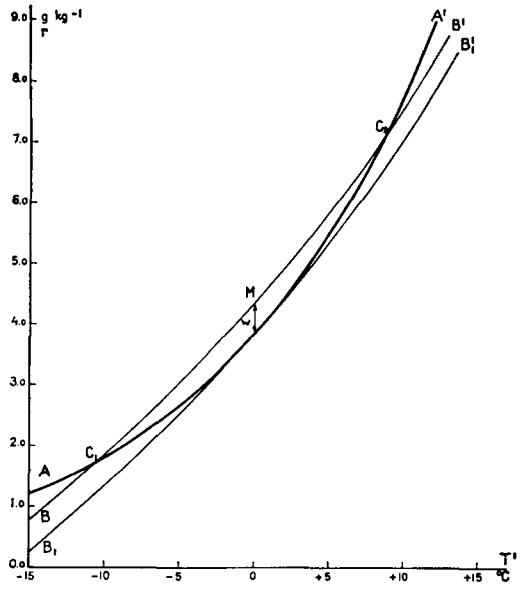


FIG. 5. $T', r$ diagram with curves ($BB'$, $B_1B_1'$) showing the interrelation between $T'$ and $r$ in a temperature transition layer.

(iii) The sensible heat of water, $cr$, is much less than the sum of the other terms of the bracket in (32). It will be deleted in what follows.

(iv) In all the formulae, the temperature is referred to the absolute scale. Since in atmospheric conditions the fraction $\theta/\theta'$ is almost equal to unity, it will be deleted in the transformations that follow from (32).

## 8. The distribution of liquid-water content in a temperature transition layer

By means of (35), we get the vertical distribution of water content at any point $(x, y)$ as a function of temperature:

$$dr = \frac{E}{H}\left[c_p + T'\frac{d}{dT'}\left(\frac{Lv'}{T'}\right)\right]dT'. \qquad (37)$$

Fig. 5 is a diagram in which the ordinate represents the water mixing ratio, the abscissa the wet-bulb temperature. The curve $AA'$ is that of the saturation-vapour mixing ratio. The area to the right of the curve represents unsaturated air, to the left saturated air with liquid drops suspended, i.e. fog. The curves $BB'$ and $B_1B_1'$ are integrals of (37) and represent the distribution of water content in relation to the temperature when the quotient $E/H$ is constant:

$$r = r_1 + \frac{E}{H}\int_{T_1'}^{T'}\left[c_p + T'\frac{d}{dT'}\left(\frac{Lv'}{T'}\right)\right]dT'. \qquad (38)$$

The integral is fixed by the boundary condition at $T_1'$ and the fraction $E/H$ or the *Bowen ratio*. For example, the conditions of a cold, wet ground surface are represented by the point $C_1$ on the saturation curve $AA'$. There, $w$ is zero. We shall discuss the reason for this later in the present section. At any other level,

$$w = v_1' - v' + \frac{E}{H}\int_{T_1'}^{T'}\left[c_p + T'\frac{d}{dT'}\left(\frac{Lv'}{T'}\right)\right]dT'. \qquad (39)$$

The integral curve cuts the curve of saturation-vapour mixing ratio not only at $C_1$ but also at $C_2$. The latter point represents the top of the fog. At the top as well as at the base, $w$ is zero. At a temperature $T_M'$ between $C_1$ and $C_2$, the water-drop mixing ratio is maximal. There the tangents of the curves $AA'$ and $BB'$ are parallel. The *Bowen ratio* $B$ is related to $T_M'$ as follows,

$$1 + B = \frac{H}{L \cdot E} = \frac{\left[c_p + T'\frac{d}{dT'}\left(\frac{Lv'}{T'}\right)\right]_M}{\left(L\frac{dv'}{dT'}\right)_M},$$

which results from (35) with $(dw/dT')_M = 0$.

In Table 1, the variation of $B$ in relation to the temperature $T_M'$ is shown.

TABLE 1.

| $T_M$ °C | $E/H$ g/cal | $B$ |
|---|---|---|
| −30 | $0.117 \times 10^{-3}$ | 12.9 |
| −25 | 0.171 | 8.56 |
| −20 | 0.243 | 5.76 |
| −15 | 0.334 | 3.94 |
| −10 | 0.444 | 2.74 |
| −5 | 0.569 | 1.93 |
| 0 | 0.708 | 1.36 |
| +5 | 0.850 | 0.98 |
| +10 | 0.992 | 0.70 |
| +15 | 1.128 | 0.51 |
| +20 | 1.25 | 0.36 |
| +25 | 1.37 | 0.26 |
| +30 | 1.46 | 0.18 |

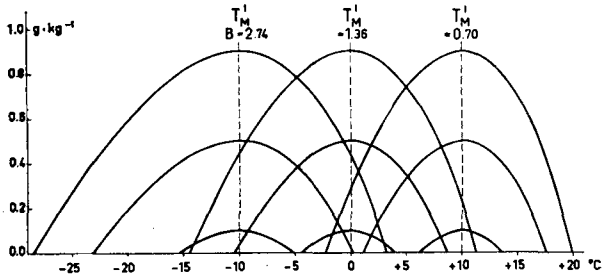


FIG. 6. Magnitude of water-drop mixing ratio in fog at different temperatures. $B$ = *Bowen ratio*. The temperature difference across the fog layer is equal to the range along the abscissa between the end points of the curves.

In ocean areas, the mean values of the *Bowen ratio* vary from $-0.2$ to $+0.5$ (SVERDRUP, 1945). The values of Table 1 refer to special conditions and are not representative of average conditions. However, in the interval from $+10°$ to $+20°$ the magnitudes agree with the empirical data.

A consequence of our assumption that water drops are transferred by eddies in the same way as vapour is that evaporation or condensation is expected to occur at the ground not only in unsaturated air but even in fog. In fog, the eddy transfer of water is not determined by the vertical gradient of vapour mixing ratio but by the gradient of total water content. It seems from the $T',r$ diagram in Fig. 5 that a difference should be found between the water contents at the top and the base when there is a temperature difference. We shall find that the latter is a vital condition for fog, so that we maintain that either evaporation or condensation always takes place at the base of fog.

The more the temperatures of the points $C_1$ and $C_2$ differ from each other, the greater is the maximum water-drop density of the fog. This is already made evident by Fig. 5, but is further illustrated by Fig. 6. In the latter figure, three sets of curves are drawn, the curves of each set having the maximum water-drop density at $-10°$, $0°$ and $+10°$C respectively. To each set, the related value of the *Bowen ratio* is added. In Fig. 7, isolines of the maximum water-drop mixing ratio are drawn in relation to the temperature $T'_M$ and the temperature difference $T'_C - T'_M$, i.e. the difference between the temperatures at the top or the base of the fog and at the maximum of drop mixing ratio. We see that the maximum water-drop mixing ratio is the greater the higher is the temperature. This appears partly from the approach of the curves to the horizontal axis at the increase of temperature, partly from the asymmetry of the curves around that axis. Thus, the lines are more crowded above the axis, where the warmer part of the fog layer is found, than below.

A scheme of the relation of vapour and liquid-water content to temperature in a steady transition layer next to a cold surface is given in Fig. 8. In part $A$, the $T',r$ diagram of Fig. 5 is found. The temperature of the cold surface is $T'_{C_1}$. The wet-bulb temperature at the top of

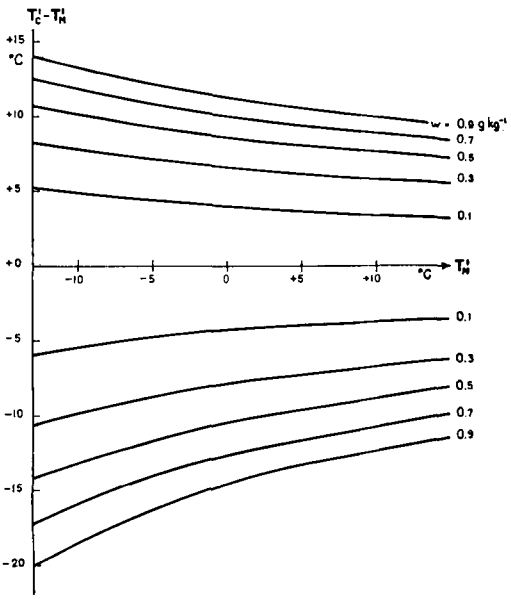


FIG. 7. The maximum of water-drop mixing ratio in fog in relation to the temperature at $M$ (Fig. 5) and the difference between this temperature and the temperature at any of the boundaries $C_1$ and $C_2$.

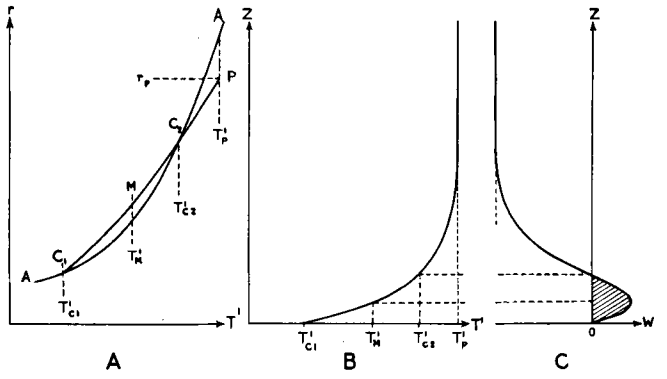


FIG. 8. The representation of the profile curves $T'$ and $w$ in the $T'$,$r$ diagram.

the transition layer is $T'_P$, the mixing ratio $r_P$. The latter is less than that of saturation. The eddy transfer of heat content as well as that of water content is directed downwards. At the ground, condensation occurs and dew is deposited. Thus, the surface is wet but no water drops can be caught by the eddies that move upwards from the surface. Hence, $w$ is zero at the surface. That is the reason why the point $C_1$ of the wet surface is put on the curve of saturation-vapour mixing ratio. It is wholly in conformity with the general practice to put the temperature of the air at a water surface equal to the temperature of the surface water.

We join the points $C_1$ and $P$ by means of an integral curve $C_1MC_2P$ of (37) and get the interrelation between water content and temperature in the transition layer. By means of the wet-bulb temperature profile, which is shown in part $B$, the distribution of water content is then deduced in part $C$. The part $C_1C_2$ of the integral curve runs to the left of the saturation curve and indicates the fog layer. It corresponds to the shaded area of positive values in the profile of liquid-water content in part $C$. The point of intersection called $C_2$ gives the top of the fog. The maximum of fog density is found at $M$, almost halfway between $C_1$ and $C_2$. Owing to the curvature of the temperature profile the level of maximum is slightly displaced to the lowest part of the fog layer.

When the air is colder than the wet surface, the point $P$ is found to the left of $C_1$ and the temperature and water content decrease upwards in the boundary layer. Also in this case, the integral curve (37) might intersect the saturation curve $AA'$ at another point $C_2$ which, however, now lies to the left of $C_1$. Indeed

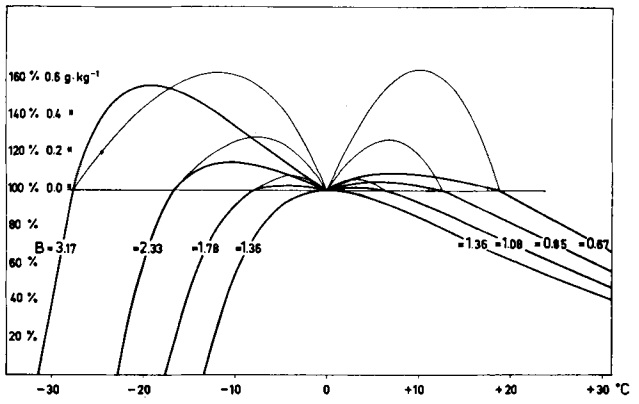


FIG. 9. The distribution of liquid-water mixing ratio (thin lines) and relative humidity in various kinds of temperature transition layers above a wet surface, of which the temperature is 0°C. *Right:* The air is warmer than the surface. *Left:* The air is colder than the surface. $B$ = *Bowen ratio.*

we know that fog occurs in the transition layer next to a warm wet surface as well as to a cold one. In the former case, evaporation takes place at the surface, in the latter case, condensation takes place.

In Fig. 9 some curves show the interrelation between water content and *dry*-bulb temperature. The temperature of the surface is arbitrarily fixed at 0°C. In the left-hand part of the diagram, the curves refer to the case where air is colder than the surface, in the right-hand part the curves exemplify cases of warm air. In the part above 100 % are drawn thin curves that give the mixing ratio of liquid water. The relative humidity is shown by the other curves. But we should rather call it the "relative content of water" since it includes liquid-water content. It exceeds 100 % in fog. Related values of the *Bowen ratio* are added to the curves.

Two features of Fig. 9 are noteworthy:

(*a*) Above the top of cold fog next to a warm underlying surface, the relative humidity decreases much more rapidly in relation to the temperature than it does above the top of warm fog.

(*b*) In a case of cold fog, the relative humidity, which includes the content of liquid water, is much greater than in the corresponding case of warm fog. The word "corresponding" implies that the temperatures of the surfaces are the same and that the temperature differences across the fog layers have the same value regardless of sign. On the other hand, the liquid-water mixing ratio of warm fog far exceeds that of a cold fog in "corresponding" cases.

## 9. The formation of advection fog

We return to formulae (32) and (33). We retain assumptions (i) to (iv) of Section 7 and add the two following ones:

(v) The density $\varrho$ of dry air is constant.

(vi) The coefficient $K$ of eddy exchange is constant.

Later, we shall add two more assumptions.

The differential equations of eddy diffusion of total heat content and total water content read

$$\varrho\left[c_p + T'\frac{d}{dT'}\left(\frac{Lv'}{T'}\right)\right]\frac{dT'}{dt} = -\frac{\partial H}{\partial z}$$

and

$$\varrho\frac{dr}{dt} = -\frac{\partial E}{\partial z},$$

respectively. Because of (32) and (33) plus assumptions (i) to (vi), the equations acquire the forms

$$\frac{dT'}{dt} = K\frac{\partial^2 T'}{\partial z^2} + K\cdot G\left(\frac{\partial T'}{\partial z}\right)^2 \tag{40}$$

and

$$\frac{dr}{dt} = K\frac{\partial^2 r}{\partial z^2}, \tag{41}$$

respectively. The symbol $G$ stands for the logarithmic derivative

$$G = \frac{1}{c_p + T'\dfrac{d}{dT'}\left(\dfrac{Lv'}{T'}\right)}\frac{d}{dT'}\left[c_p + T'\frac{d}{dT'}\left(\frac{Lv'}{T'}\right)\right]. \tag{42}$$

If we want an explicit form of the differential equation for integration of the liquid-water content, we may substitute $v' + w$ for $r$ in (41),

$$\frac{dw}{dt} + \frac{dv'}{dT'}\cdot\frac{dT'}{dt} = K\frac{\partial^2 w}{\partial z^2} + K\frac{d^2 v'}{dT'^2}\left(\frac{\partial T'}{\partial z}\right)^2 + K\frac{dv'}{dT'}\frac{\partial^2 T'}{\partial z^2}.$$

We recall that $v'$ only depends on the wet-bulb temperature. In combination with (40), the equation is shortened to

$$\frac{dw}{dt} = K\frac{\partial^2 w}{\partial z^2} + K\left[\frac{d^2 v'}{dT'^2} - G\frac{dv'}{dT'}\right]\left(\frac{\partial T'}{\partial z}\right)^2. \tag{43}$$

The object of the present section is to show the role played by turbulence in the procedure of fog formation. It is not intended to set out the exact quantity of water drops that results from our theory. We already gave up that aim when we made assumption (vi). That assumption is absolutely contrary to well-known facts of the vertical variation of the coefficient of eddy exchange, but it simplifies the theoretical discussion considerably.

We shall discuss some more assumptions that aim to simplify the mathematical discussion as far as possible:

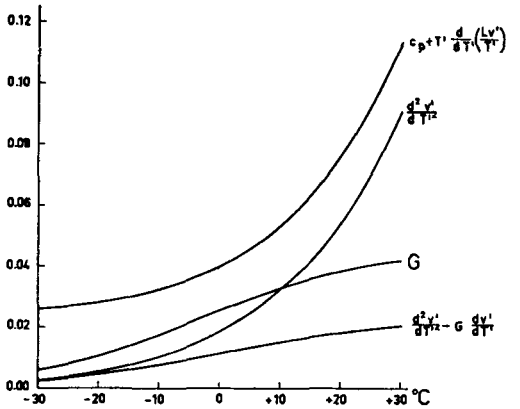


FIG. 10. The variations of some functions of the first and second derivatives of $v'$. The units of the ordinates of $c_p$, $d^2v'/dT'^2$ and $G$ are respectively 10 cal/(g °C), g/(kg °C²) and °C⁻¹. The functions are based on the values of $v'$ at atmospheric pressure 1000 mbs.

(vii) The function

$$c_p + T' \frac{d}{dT'}\left(\frac{Lv'}{T'}\right)$$

is constant, i.e. $G = 0$.

(viii) The derivative $d^2v'/dT'^2$ is constant.

Fig. 10 shows the strict variations of the functions mentioned in (vii) and (viii). In addition, there are found the variations of $G$ and

$$\frac{d^2v'}{dT'^2} - G\frac{dv'}{dT'}.$$

The first term in the right-hand member of (40) settles the principal variations of $T'$. The second term brings about minor additional variations that are due to $G$, i.e. the variation of the specific heat in the form of (27).

We see in Fig. 10 that the variation of $G$ is relatively small along the range of the abscissa. We get an approximate form of (40) that is more easy to integrate than the original differential equation when we replace $G$ by a constant. We fit the constant to the average of $G$ in the relevant temperature interval.

We assume that

$$T' = T'_0 + \Delta T'_0 \phi(x,y,z,t), \qquad (44)$$

where $T'_0$ and $\Delta T'_0$ are constants of integration, is the complete integral of a differential equation that contains the predominant terms of (40) only, namely the equation:

$$\frac{dT'}{dt} = K\frac{\partial^2 T'}{\partial z^2}. \qquad (45)$$

Still for the purpose of simplifying the integration of (40), we put the integral (44) into the secondary term of (40):

$$\frac{dT'}{dt} = K\frac{\partial^2 T'}{\partial z^2} + K \cdot G(\Delta T'_0)^2\left(\frac{\partial \phi}{\partial z}\right)^2. \qquad (46)$$

It is easily verified that

$$T' = T'_0 + \Delta T'_0 \phi + \tfrac{1}{2} G(\Delta T'_0)^2 \phi(1-\phi) \qquad (47)$$

is the complete integral of (46). $T'_0$ and $\Delta T'_0$ are constants of integration. (47) may with good approximation be used instead of the relevant integral of (40).

We see in Fig. 10 that the variation of

$$\frac{d^2v'}{dT'^2} - G\frac{dv'}{dT'}$$

is relatively small. We replace it in (43) by a constant factor that is identical with the average in the range of its variation, and $\partial T'/\partial z$ by the derivative of (44). Then,

$$w = w_1\phi + w_2(1-\phi) + \frac{1}{2}\left[\frac{d^2v'}{dT'^2} - G\frac{dv'}{dT'}\right](\Delta T'_0)^2\phi(1-\phi) \qquad (48)$$

is an approximate form of the complete integral of (43). The coefficients $w_1$ and $w_2$ are constants of integration.

Now, the consequences of the assumptions (vii) and (viii) become clear. The first one is that in (46) and (47) the last term will be omitted. But then there results a value of $T'$ that is up to $\frac{1}{2}G(\Delta T_0')^2$ too low in a temperature range between $T_0'$ and $T_0' + \Delta T_0'$. For example, at about 0°C, $G$ is 0.025°C$^{-1}$. The error of $T'$ on account of (vii) is less than 0.3°C when $\Delta T_0' \leqslant 10$°C.

Further, assumption (vii) implies that in (43) and (48),

$$\left[\frac{d^2v'}{dT'^2} - G\frac{dv'}{dT'}\right]$$

will be replaced by $d^2v'/dT'^2$. Since the latter is greater than the former, $w$ is overestimated on account of (vii). At 0°C, the difference between the factors in question is 0.007 $10^{-3}$ °C$^{-2}$ and the maximum error that we get in $w$ on account of (vii) is 0.09 $10^{-3}$ when $\Delta T_0' \leqslant 10$°C.

The forms of the curves in Fig. 5 give another view of the consequence of assumptions (vii) and (viii). On account of the latter, the curve $AA'$ of the saturation mixing ratio is adapted to a parabolic curve. Because of the former, the integral curves $BB'$ and $B_1B_1'$ get the form of straight lines, as is easily proved by means of the differential equation (37).

The representation of $BB'$ and $B_1B_1'$ by means of straight lines recalls Fig. 4, which illustrates the effect of the mixing of two masses of damp air as explained by TAYLOR (1917), BRUNT (1935) and earlier writers mentioned in Section 4. Assumption (vii) implies that we consider the specific heat of saturated air as constant. That is in practice the same as saying that we disregard the release of latent heat. The temperature and liquid-water content of the mixture are then represented by point $B$ in Fig. 4. We recall that the temperature is found by means of (47), the water content by means of (48). The equations are adapted to the condition of (vii) by omitting the terms containing $G$.

On the other hand, if regard is paid to the release of latent heat, the terms containing $G$ must be retained and added to the values of temperature and liquid-water content at $B$. This implies that the representation of the mixture is removed from $B$. The temperature and the *vapour* content are now found at $D$.

But the *total water* content of the mixture is still found at $B$. In contrast to Brunt, we attribute to the ordinate the total water content instead of the vapour content or the vapour pressure. From our point of view, the water content in the mixture remains that of $B$, irrespective of whether condensation occurs or not. Hence, we find the mixture to be represented by the intersection between the horizontal line through $B$ (representing the water content) and the vertical line through $D$ (representing the temperature).

The curve $BB'$ in Fig. 5 is the locus of the intersection in Fig. 4 between the horizontal line through $B$ and the vertical line through $D$ at variable proportions by weight of the two masses mixed.

Brunt discusses the slope of the line $BD$ and shows that its tangent of inclination to the $T$-axis is approximately $-c_p/L$. The value of this fraction is $-0.390$ $10^{-3}$ at $-30$°C and $-0.415$ $10^{-3}$ °C$^{-1}$ at $+30$°C.

Regardless of sign, the tangent of inclination of $BD$ is equal to the quotient of the vertical projection of $BD$, i.e. $w$ in (48), and its horizontal projection, i.e. the last term in (47). The line $BD$ is relevant only to such mixtures as are saturated by vapour. Accordingly, we bound $w$ in (48) to positive and zero values within $0 \leqslant \phi \leqslant 1$ by putting $w_1 = w_2 = 0$.

After equal terms in the numerator and the denominator of the quotient in question have been deleted, we get the formula:

$$\textit{Tangent of inclination of } BD \textit{ to the axis of } T \text{ (Fig. 4)} = \frac{dv}{dT} - \frac{1}{G}\frac{d^2v}{dT^2}.$$

The second term is the predominant one in the formula. By putting $G$ in the approximate form $(L/c_p)(d^2v/dT^2)$, we find that the term is related to Brunt's version mentioned above. Without any approximation, our formula gives $-0.415$ $10^{-3}$ °C$^{-1}$ at $-30$°C and $-0.490$ $10^{-3}$ °C$^{-1}$ at $+30$°C.

Like Fig. 9, Fig. 11 shows the variation of water-drop content in the boundary layer above a surface. The fully drawn curves are based on strictly correct curves $AA'$ and $BB'$ in Fig. 5 but the dashed curves show the variation that results if $AA'$ is adapted to a parabolic curve and $BB'$ and $B_1B_1'$ to straight lines. Again we find that assumptions (vii) and (viii) result in

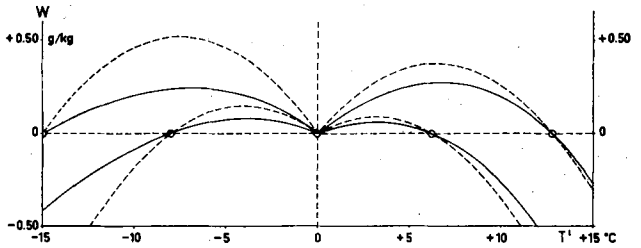


FIG. 11. The distribution of the liquid-water mixing ratio in four kinds of temperature transition layers adjacent to a wet surface. Like the curves of Fig. 9, the *continuous curves* are based on the differential equation (37) without any approximation. In the computation of the *dashed curves*, the variations of

$$\left[c_p + T' \frac{d}{dT'}\left(\frac{Lv'}{T'}\right)\right] \quad \text{and} \quad \frac{d^2v'}{dT'^2} \quad \text{are disregarded.}$$

an overestimation of the liquid-water content at fixed conditions at the base and at the top of the fog. This shortcoming will be inherent in the following discussions of the principles of advection fog and radiation fog.

We would stress that the aim of this section and the next is not to find the exact quantity of liquid-water content in fog but rather to give a presentation of the fundamentals of fog formation. The liquid-water content of fog was discussed in Section 8 and shown in Figs. 6, 7 and 9. At present, we want the simplest differential equations that will give a basic understanding of fog formation.

Now, we fix the advective formation of fog to the following boundary conditions, which are illustrated in Fig. 12:

1. There is a horizontal flow of air perpendicular to a line of discontinuity at the ground surface. We put the $x$-axis in the direction of the air flow and the intersection of the line of discontinuity at $x = 0$. The wind velocity is called $u$.

2. At $x = 0$ and $z \geqslant 0$: $T' = T_0'$ and $r = v_0' + w_0$. We assume that the air is unsaturated upstream of the line of discontinuity, i.e. $w_0 < 0$.

3. At $x > 0$ and $z = 0$: $T' = T_0' + \Delta T_0'$ and $w = 0$. Downstream of the line of discontinuity, the surface is wet. Its temperature differs abruptly from that of the surface upstream.

The partial differential equations (40) and (43) fit the problem in the following approximate forms:

$$u \frac{\partial T'}{\partial x} = K \frac{\partial^2 T'}{\partial z^2} \tag{49}$$

and

$$u \frac{\partial w}{\partial x} = K \frac{\partial^2 w}{\partial z^2} + K \frac{d^2 v'}{dT'^2} \left(\frac{\partial T'}{\partial z}\right)^2. \tag{50}$$

Adapted to the boundary conditions, the particular integral of (49) reads

$$T_1' = T_0' + \Delta T_0' \frac{2}{\sqrt{\pi}} \int_{z\sqrt{\frac{u}{4Kx}}}^{\infty} e^{-\eta^2} d\eta \tag{51}$$

and the particular integral $\phi$ in (44) gets the form

$$\phi(x, z) = \frac{2}{\sqrt{\pi}} \int_{z\sqrt{\frac{u}{4Kx}}}^{\infty} e^{-\eta^2} d\eta. \tag{52}$$

The deduction is found in textbooks on partial differential equations, for example WEBER (1912).

A particular integral of (50) is found by means of putting $G = 0$ in (48) and reads, when the constants of integration are adapted to the boundary conditions of advective fog formation,

$$w = w_0 (1 - \phi) + \tfrac{1}{2} (\Delta T_0')^2 \frac{d^2 v'}{dT'^2} (1 - \phi) \phi. \tag{53}$$

With reference to (53), the drawing of Fig. 12 shows the distribution of liquid-water content in the air downstream of the line of discontinuity. First, there are four profile curves showing the vertical distribution at four distances downstream. The shaded areas represent the fog in the transition layer. Secondly, four isolines, each related to a fixed value of $w$, illustrate the vertical diffusion of liquid-water content. The heights of the isolines increase with the square root of the distance from the line of disconti-

nuity. For example, the level of maximum water-drop density is determined by $z_{max}$, which is fixed by the relation

$$\phi(x, z_{max}) = \tfrac{1}{2}\left[1 - \frac{2w_0}{(\Delta T_0')^2 \dfrac{d^2 v'}{dT'^2}}\right].$$

Since $\phi = \frac{1}{2}$ at $z = 0.48\sqrt{4Kx/u}$, $z_{max}$ is less than $0.48\sqrt{4Kx/u}$ when $w_0 < 0$.

The maximum of water-drop mixing ratio is

$$w_{max} = \frac{1}{8}\left[1 + \frac{2w_0}{(\Delta T_0')^2 \dfrac{d^2 v'}{dT'^2}}\right]^2 (\Delta T_0')^2 \frac{d^2 v'}{dT'^2}.$$

It is interesting to find that the maximum value is independent of the distance of flow from the line of discontinuity. The maximum is established immediately downstream. Thus it is a characteristic feature of advection fog that the height of the top of the fog increases but the maximum value of liquid-water content is retained downstream.

In Fig. 12, nothing is presumed about the sign of the temperature change across the line of discontinuity. In fact, the sign of $\Delta T_0'$ does not affect the main form of the profile of liquid-water content. The sign is cancelled, since $\Delta T_0'$ is squared in (53). Thus, the drawing of the figure is applicable to the formation of *cold-air advection fog* (e.g. steam fog) as well as *warm-air advection fog* (e.g. fog adjacent to a thawing snow surface).

In Fig. 13, another example of advective fog formation is given. The profile curves of dry-bulb and wet-bulb temperatures are added,

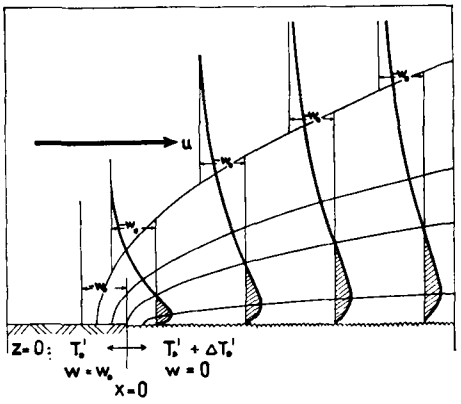


FIG. 12. Diagrammatic presentation of the growth of advection fog on the lee side of a shore line.

but otherwise the figure does not seem to need any explanation in addition to that given to the preceding figure. The units of the abscissa refer to Fig. 16, and we shall return to Fig. 13 in the discussion of radiation fog.

The slopes of the parabolic curves in Fig. 12 show the rate of growth of the height of the fog downstream of the line of discontinuity. The parabolic curves are specified by equations of the form

$$z^2 = \text{const}\,\frac{4K}{u}x \qquad (54)$$

with different constants. Their slopes depend on the coefficient $K$ of eddy exchange and the wind velocity $u$,

$$\frac{dz}{dx} = \frac{1}{2}\,\text{const}\,\sqrt{\frac{4K}{u}}\cdot\frac{1}{\sqrt{x}}. \qquad (55)$$

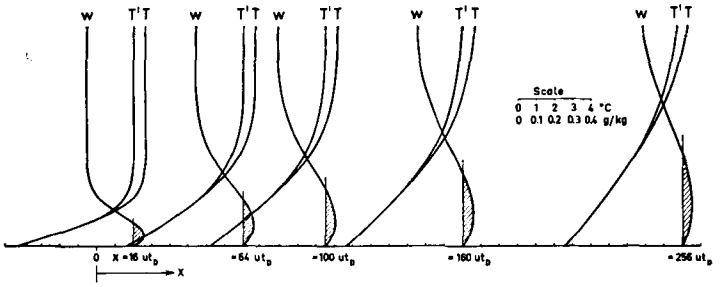


FIG. 13. Profiles of $T$, $T'$ and $w$ computed by means of (49) and (50). The unit of the horizontal distance refers to formation of radiation fog exemplified in Fig. 16. In the present figure the temperature at the surface is constantly equal to the surface temperature in the fourth stage ($t = 160\ t_D$) of Fig.16. The conditions of the unmodified air at the top are the same in both figures.

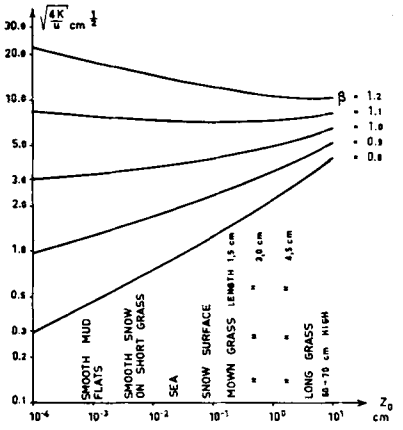


FIG. 14. The growth of height of advection fog (in terms of $\sqrt{4K/u}$) as a function of roughness parameter ($z_0$) at different thermal stratifications ($\beta < 1$ at stable stratification, $\beta > 1$ at unstable stratification).

These two concepts depend both on the thermal stratification of the boundary layer and the roughness of the ground. In order to show this, we introduce the very simple form of wind profile verified by DEACON (1953),

$$\frac{u}{u_*} = \frac{1}{k(1-\beta)}\left[\left(\frac{z}{z_0}\right)^{1-\beta} - 1\right]. \qquad (56)$$

The meaning of the symbols is the common one:

- $u_*$ is the *frictional velocity* fixed by the frictional stress,
- $k$ is *von Karman's constant* and
- $z_0$ the *roughness length*.
- $\beta$ is smaller than unity in stable but greater than unity in unstable stratifications.

By substitution of *Taylor's series* for $e^{(1-\beta)\cdot \log z/z_0}$ and putting $\beta = 1$, it may be shown that (56) gets the well-known logarithmic form, characteristic of neutral stability conditions,

$$\frac{u}{u_*} = \frac{1}{k} \log \frac{z}{z_0}.$$

On the basis of (56), the coefficient of eddy exchange reads

$$K = k u_* z \left[\frac{z}{z_0}\right]^{\beta - 1},$$

and we get for the desired term the equation

$$\sqrt{\frac{4K}{u}} = 2k\left[\frac{z(1-\beta)}{\left(\frac{z}{z_0}\right)^{1-\beta}\left[\left(\frac{z}{z_0}\right)^{1-\beta} - 1\right]}\right]^{\frac{1}{2}}. \qquad (57)$$

In neutral stability conditions, (57) reads

$$\sqrt{\frac{4K}{u}} = 2k\sqrt{z}\left[\log \frac{z}{z_0}\right]^{-\frac{1}{2}}.$$

Equations (56) and (57) show that the rate of growth of fog depends partly on the roughness ($z_0$) of the ground surface and partly on the thermal stratification ($\beta$) of the air.

In Fig. 14, some isolines, which refer to fixed values of $\beta$, show the relation of (57) to roughness and stratification. The abscissa as well as the ordinate are drawn on a logarithmic scale. The different slopes of the five isolines show that (57) is very sensitive to changes of roughness at stable stratification. In neutral conditions there is still a trend, but in unstable conditions hardly any remarkable variation is found. Along the abscissa, some examples of reference of $z_0$ to natural types of ground surfaces are quoted from the paper of Deacon. If we compare the case of $z_0 = 0.1$ cm with that of $z_0 = 0.001$ cm, we find that at moderate stability (e.g. $\beta = 0.9$) the rate of growth of the fog in the former case is almost twice as great as in the latter. The difference becomes more striking with greater stability.

It should be mentioned that the figures along the abscissa of Fig. 14 refer to $z = 2$ m. The values of $K$ and $u$ in (54) represent average conditions in the range of integration of the differential equations (49) and (50). That means that the curves of the figure are representative of a case where the averages of the vertical variations of $K$ and $u$ are equal to the values that are found at a height of 2 m above the surface. In the alternative of another height, for example 20 m, the figures and the legends of $z_0$ along the abscissa should be shifted one step to the left, i.e. $10^{-3}$ should be substituted for $10^{-4}$, $10^{-2}$ for $10^{-3}$, etc.—or the curves should be shifted correspondingly to the right. However, the transformation does not change any of the features of the diagram that were essential for our conclusion. Thus, the conclusions seem to have general validity for a surface boundary layer and can be summed up as follows.

First, unstable stratifications ($\beta > 1$) are expected to bring about a more rapid increase of the height of advection fog than stable ones ($\beta < 1$). This is already implied by the sense of stability but is also made evident by Fig. 14. Secondly, the downstream increase of the height is at stable stratification expected to be remarkably sensitive to the roughness of the ground. The second conclusion is not so self-evident as the first and seems hitherto not to have been pointed out. We know that steam fog is formed in winter in strong inversions of cold air over a river that is free of ice. The present author has observed that such fog simultaneously extends to quite different heights at neighbouring places. From a theoretical point of view, the surface roughness seems to be the principal cause of this variation.

During the years 1950–52, members of the Institute of Low Temperature Science in Japan collaborated in an investigation on the advection fog which in spring and summer frequently invades the south-eastern shore of Hokkaido. It is formed in the region of the ocean where *Oyashio*, the cold current, and *Kuroshio*, the warm current, come in contact with each other. The chief object of the investigation was the estimation of the role played by the forest along the coast in capturing the fog.

Many of the members of the team contributed investigations that have interest outside the scope of the object we mentioned. Very interesting are the measurements by KUROIWA & KINOSITA (1953) and KUROIWA (1953). They investigated the vertical distribution of liquid-water content in fog. In the foregoing, we have assumed that the liquid-water content is zero at the base of fog. This vertical approach is verified by the profiles reproduced in the papers just referred to. We also wish to mention the contribution of IMAHORI (1953), who puts forward a theory on the vanishing mechanism of advection fog and takes into consideration both the diffusion of the droplets and their mean downward motion caused by the gravitational force. He integrates a partial differential equation that in terms of our notations (50) has the form

$$u\frac{\partial w}{\partial x} = K\frac{\partial^2 w}{\partial z^2} + \mu u\frac{\partial w}{\partial z}.$$

The difference between Imahori's differential equation and ours (50) is that Imahori neglects the effect of the curvature of the saturation curve but pays regard to the gravity effect. The coefficient $\mu u$ is the mean downward velocity of the droplets. It varies with the size of the drops. Imahori puts for it the average velocity of the most frequent size of drops found in the fog at the coast of Hokkaido, i.e. 1.3 cm sec$^{-1}$, corresponding to a radius of 0.01 mm. The result of Imahori's investigation is that the gravity effect is found to be trivial within limited ranges of height ($z$) above the surface and distance ($x$) from the shore.

We are interested to know which of the terms mentioned above is the greater one, namely the one which is due to the gravity or that which is due to the curvature of the saturation curve. The quotient of the two reads

$$\mu u\frac{\partial w}{\partial z} : K\frac{d^2 v'}{dT'^2}\left(\frac{\partial T'}{\partial z}\right)^2 = \mu\sqrt{\frac{ux}{K}}\,(1-2\phi)\left(\frac{\partial \phi}{\partial \alpha}\right)^{-1},$$

where $w$ is put in the integral form (53) with $w_0 = 0$ and

$$\alpha = z\sqrt{\frac{u}{4Kx}}$$

We put $K = 10^4$ cm$^2$ sec$^{-1}$, $u = 500$ cm sec$^{-1}$ and $\mu u = 1.3$ cm sec$^{-1}$. We find that the quotient varies as follows:

When $x = 10$ m, between $+0.02$ at $z = 0$ m and $-1.00$ at $z = 6$ m.
When $x = 100$ m, between $+0.05$ at $z = 0$ m and $-1.00$ at $z = 15$ m.
When $x = 1$ km, between $+0.16$ at $z = 0$ m and $-1.00$ at $z = 39$ m.

Within these ranges of $z$, the effect of the curvature of the saturation curve is greater than that of gravity. It should be mentioned that the level of the maximum liquid-water content, where the gravity effect is zero, is always found within the range of $z$ mentioned. Imahori shows that the level of maximum liquid-water content is slightly lowered because of the gravitational force. Since the chief object of our study is the procedure of fog formation that takes place immediately downstream $x = 0$ and adjacent to the surface $z = 0$, we are allowed to

disregard the gravity effect and we did in fact do so.

Lastly, we wish to mention a theoretical investigation by TIMOFEEV (1955). He discusses the procedure of advective fog formation by means of the differential equations

$$u\frac{\partial T}{\partial x}=\frac{\partial}{\partial z}\left(K\frac{\partial T}{\partial z}\right) \quad \text{and} \quad u\frac{\partial r}{\partial x}=\frac{\partial}{\partial z}\left(K\frac{\partial r}{\partial z}\right)$$

and integrates them with a variable function of the coefficient of eddy exchange. His interest is chiefly directed towards the relation of the humidity and the temperature in the unmodified air on the one hand to a definite value of liquid-water content in the fog (0.1 $g\,m^{-3}$) on the other. He does not touch on the mixing role played by turbulence or on the thermodynamics of saturated air. It is, however, important that we should know the latter before we apply the above-mentioned differential equations of diffusion to fog conditions. By doing so, we have proved that it is not the dry-bulb temperature but the wet-bulb temperature that should be put into the differential equations.

## 10. The formation of radiation fog

The starting process of radiation fog formation is the black-body radiative cooling of the ground and the simultaneous convective heat loss in the air adjacent to the ground surface. At a next stage, the density of the fog is increased so much that the black-body emissivity of the drops becomes effective and the fog takes over a part of the role of cooling medium initially played by the ground.

The present section will be devoted to the first stage of the process of fog formation. The effect of radiative cooling of the drops will be discussed in the next section. However, it should here be pointed out that the latter effect should not be disregarded in a discussion of the complete problem of radiation fog formation, since the growth of height of the fog is not only a result of convection and diffusion but also of the rise of the level of radiative cooling.

Thus, the problem that we are faced with first of all is to find the variations of temperature and humidity, i.e. of

$$T' = T'(z,t) \text{ and}$$
$$r = r(z,t)$$

in relation to the radiative heat loss at the ground. It implies that we have to solve the forms

$$\frac{\partial T'}{\partial t}=K\frac{\partial^2 T'}{\partial z^2} \tag{58}$$

and

$$\frac{\partial r}{\partial t}=K\frac{\partial^2 r}{\partial z^2} \tag{59}$$

of the differential equations (40) and (41). Equation (58) is subject to $G=0$. The consequence of this is discussed in Section 9. The integral of (58) should be fixed to a boundary condition that gives the decrease of surface temperature in relation to the radiative heat loss.

BRUNT (1944) has used the differential equation (58), but with reference to the dry-bulb temperature, for a discussion of the cooling rate of the ground surface when the net radiative loss of heat is initially zero but momentarily jumps up to a certain value and then remains constant. He got the result that the fall of surface temperature is proportional to the square root of the time that has passed since the moment that radiative heat loss started,

$$T(0,t) = T(0,0) - N\sqrt{t}, \tag{60}$$

where $N$ is a constant.

Brunt based his discussion on the assumption that there is a constant supply of sensible heat through the conductivity of the ground. He neglected the eddy heat transfer of the air. However, the square-root time variation of the surface temperature will follow whether the radiative heat loss is assumed to be balanced by the heat conductivity of the ground, or by the eddy heat transfer of the air, or—a third possibility, which is close to the real conditions—by the conductivity of the ground *and* the eddy transfer of the air. In the following discussion, we shall pay principal attention to the eddy transfer and leave out of consideration the heat supply of the ground. However, we should still bear in mind that the constant of (60) greatly depends on the latter factor and is the greater the poorer is the conductivity of the ground. Furthermore, it is the greater the greater is the net radiative loss of heat at the surface.

In the present problem of fog formation, our interest in the ground surface is directed to the question whether it is dry or wet. We attach to these alternatives the following characteristics:

A *dry* surface is expected neither to absorb nor emit any vapour. Consequently, it does not affect the vapour mixing ratio of the air, and the latter is constant throughout the boundary layer above a dry surface. A rock might be a good example of such a surface.

On the other hand, we assume that a *wet* surface is covered by a liquid film and that evaporation and condensation take place there. The eddies that start moving upwards at the surface cannot catch any water drops but are saturated by vapour due to molecular diffusion, in the same way as they take on the temperature of the surface by molecular conduction. In view of this, we put the water-drop content of the air at the wet surface equal to zero and the temperature there equal to that of the surface.

Further, the wet surface does not absorb any vapour. In consequence, it does not receive any latent heat. The latent part of the downward eddy transfer of total heat content is completely converted into sensible heat at the wet surface by condensation. For the same reason, the whole latent part of the heat received by the air at the surface is brought about by evaporation.

The well-known definition of the *dew-point* temperature of the air implies that the temperature of a dry surface exceeds the dew point. When the surface temperature is below the dew point, the surface is never dry. A wet surface may, however, be either warmer or colder than the dew point. If it is warmer, there should be a reserve of water for evaporation. We have already met that alternative, in the case of steam fog formation, in Section 9.

First, *in unsaturated air over a dry surface*, the eddy transfer of latent-heat content is zero, since there is no vertical variation of water content. Consequently, the transfer of sensible-heat content is identical with the *total* heat content transferred. That means that the heat transfer over a dry surface is equally well estimated by means of the dry-bulb temperature as by means of the wet-bulb,

$$H = -\varrho c_p K \frac{\partial T}{\partial z}$$

$$= -\varrho K \left[ c_p + cr + T' \frac{d}{d T'} \left( \frac{L v'}{T'} \right) \right] \frac{T}{T'} \frac{\partial T'}{\partial z}. \qquad (61)$$

Secondly, *in unsaturated air over a wet surface* the temperature of which is below the dew point, there is a net downward transfer of vapour, since the mixing ratio $r$ decreases downwards. Vapour is condensed at the surface, and a part of the total heat content exchanged is formed of latent heat. Thus, the eddy transfer of total heat content is represented by the wet-bulb part of (61) but not by the dry-bulb formula.

Summing up, we find that we may use the partial differential equation (58) for estimation of the temperature variation in a boundary layer whether this is adjacent to a dry surface or a wet surface, provided however that we use the wet-bulb temperature as prescribed.

Since we use the wet-bulb temperature instead of the dry-bulb, the boundary condition (60) should be written in terms of the wet-bulb temperature, too. On a wet surface this is no problem, since there the wet-bulb temperature is identical with the dry-bulb temperature. For a dry surface, equation (20) gives the dry-bulb temperature in terms of the wet-bulb,

$$T(0, t) = T'(0, t) + \frac{L}{c_p + c_p' r} [v'(0, t) - r].$$

As already pointed out, $r$ is expected to remain constant adjacent to a dry surface. Hence,

$$\frac{\partial T}{\partial t} = \frac{\partial T'}{\partial t} \left[ 1 + \frac{L}{c_p + c_p' r} \frac{d v'}{d T'} \right]. \qquad (62)$$

This formula is valid when the surface is dry, which happens between $T'(0,0)$ and the dew point. We shall find that this interval is mostly only a small part of the total range of temperature variation at radiation fog formation. In consequence, the variations of $dv'/dT'$ may be disregarded in (62). Otherwise, we do not neglect the variations of this derivative.

Thus, we may transform (60) into the conditions of the wet-bulb temperature by substitution of $N'$ for $N$, where

$$N = N' \left[ 1 + \frac{L}{c_p + c_p' r} \cdot \frac{d v'}{d T'} \right]. \qquad (63)$$

In the light of the foregoing definitions and explanations we fix the boundary conditions of our problem of radiation fog formation as follows:

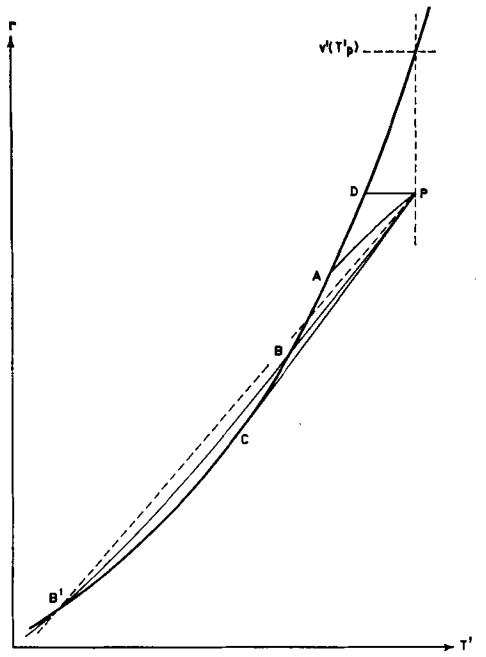


FIG. 15. The interrelation between $T'$ and $r$ at the formation of radiation fog. $P$ = state of the unmodified air. $D$ = dew point. $A$, $C$ and $B'$ are temperatures at the base of the fog in successive stages of radiative cooling. The thin lines $PA$, $PC$ and $PBB'$ represent the interrelation between $T'$ and $r$ in the transition layer. The dashed curve $PB'$ relates to a steady surface temperature.

1. When $t = 0$ and $z \geq 0$:
   $T' = T'_P$, i.e. the wet-bulb temperature of the unmodified air.
   $r = r_P$, i.e. the vapour mixing ratio of the unmodified, unsaturated air.

2. When $0 < t \leq t_D$, the surface at $z = 0$ is dry:
   $T'(0,t) = T'_P + f(t) \geq T_D$,
   where $f(t) = -N'\sqrt{t} < 0$.
   $T_D$ is the dew point of the air.
   $r = r_P$, i.e. the vapour mixing ratio remains equal to that of the unmodified air.

3. When $t_D < t$, the surface at $z = 0$ is wet:
   $T'(0,t) = T'_P + f(t) < T_D$
   $w = 0$.

We shall treat the periods of dry and wet surfaces separately. Thus, there is first the period:

$0 \leq t \leq t_D$

In Fig. 15, which is a $T', r$ diagram, the point $P$ refers to the conditions of the unmodified air. The dew point of the air is found at the point $D$ having the ordinate $r_P$ and lying on the saturation curve.

In radiative heat loss, the temperature of the surface and of the air above it decreases but the total water content $r$ remains constant. Hence, the locus of interrelation between $T'$ and $r$ in the boundary layer is the horizontal line $PD$. By integration of (58), we find for the temperature profile above the surface

$$T'(z,t) = T'_P + \frac{2}{\sqrt{\pi}} \int_{\frac{z}{\sqrt{4Kt}}}^{\infty} f\left(t - \frac{z^2}{4K\eta^2}\right) e^{-\eta^2} d\eta. \quad (64)$$

Recalling the identity of $f(t)$ with a square-root function, we transform (64) into

$$T'(z,t) = T'_P + \frac{2}{\sqrt{\pi}} f(t) \int_{\frac{z}{\sqrt{4Kt}}}^{\infty} \sqrt{1 - \frac{z^2}{4Kt\eta^2}}\, e^{-\eta^2} d\eta. \quad (65)$$

For simplification of the notation, we introduce the function

$$Y_n(\alpha, \varkappa) = \frac{2}{\sqrt{\pi}} \int_{\alpha \cdot \varkappa}^{\infty} \left(1 - \frac{\alpha^2}{\eta^2}\right)^n e^{-\eta^2} d\eta. \quad (66)$$

The integral of the last term in (65) is represented in (66) if we put $n = \frac{1}{2}$, $\alpha = z/\sqrt{4Kt}$ and $\varkappa = 1$. By means of a somewhat lengthy transformation, given in Appendix B, the last-mentioned integral assumes the more elementary form

$$Y_{\frac{1}{2}}(\alpha, 1) = \frac{2}{\sqrt{\pi}} \int_{\alpha}^{\infty} \sqrt{1 - \frac{\alpha^2}{\eta^2}}\, e^{-\eta^2} d\eta$$

$$= e^{-\alpha^2} - 2\alpha \int_{\alpha}^{\infty} e^{-\eta^2} d\eta. \quad (67)$$

It was noted that the vertical distribution of vapour remains constant up to the moment when the temperature of the surface reaches the

dew point. Thus, no vertical variation of mixing ratio appears before that. The liquid-water deficit, however, decreases owing to the approach of the wet-bulb temperature to the dew point,

$$-\omega = v'(T') - r_P = v'(T') - v'(T_D). \qquad (68)$$

The saturation-vapour mixing ratios at any two temperatures may be put in relation to each other by means of *Taylor's series*,

$$v'(T') = v'(T'_P) + \left(\frac{dv'}{dT'}\right)_P (T' - T'_P) + \frac{1}{2}\frac{d^2 v'}{dT'^2}(T' - T'_P)^2. \qquad (69)$$

We recall that $d^2v'/dT'^2$ is assumed to be constant. We refer to assumption (viii) in Section 9.

By application of (69) to (68), we get

$$-w = -w_P + \left(\frac{dv'}{dT'}\right)_P (T' - T'_P) + \frac{1}{2}\frac{d^2 v'}{dT'^2}(T' - T'_P)^2. \qquad (70)$$

We get the dew point $T_D$ if we put the right-hand member of (70) equal to zero. We find that the dew point is fixed by the liquid-water deficit $-w_P$ and the wet-bulb temperature $T'_P$.

When the dew point is reached at the surface, the surface is moistened and we enter then ext period.

$t > t_D$

The net loss of radiative heat remains unchanged and the fall of the wet-bulb temperature at the surface goes on at the same rate before and after $t_D$. Equation (64) remains valid for the wet-bulb temperature profile in the boundary layer next to the surface.

In contrast to the continuous fall of the wet-bulb temperature, there is discontinuity in the fall of the dry-bulb temperature at time $t_D$ since the latent-heat content then becomes an effective part of the total heat transferred and reduces the part of sensible-heat content transferred.

The air is now saturated by vapour at the surface and $w$ is there steadily zero. In consequence, the water content of the air at the surface decreases along the saturation curve $DABCB'$ in Fig. 15, and it is easily related to the mixing ratio at the dew point by means of *Taylor's series*,

$$r(0, t) = r_P + \left(\frac{dv'}{dT'}\right)_D [T'(0, t) - T_D] + \frac{1}{2}\frac{d^2 v'}{dT'^2}[T'(0, t) - T_D]^2$$

$$= r_P + \left(\frac{dv'}{dT'}\right)_D [f(t) - f(t_D)] + \frac{1}{2}\frac{d^2 v'}{dT'^2}[f(t) - f(t_D)]^2. \qquad (71)$$

We get the vertical distribution of the total water content in the boundary layer by integration of (59). Having regard to the boundary condition in the form of (71), the particular integral reads

$$r(z, t) = r_P + \left(\frac{dv'}{dT'}\right)_D \cdot \frac{2}{\sqrt{\pi}} \int_{\frac{z}{\sqrt{4K(t-t_D)}}}^{\infty} \left[f\left(t - \frac{z^2}{4K\eta^2}\right) - f(t_D)\right] e^{-\eta^2} d\eta + \frac{1}{2}\frac{d^2 v'}{dT'^2} \cdot \frac{2}{\sqrt{\pi}} \int_{\frac{z}{\sqrt{4K(t-t_D)}}}^{\infty} \left[f\left(t - \frac{z^2}{4K\eta^2}\right) - f(t_D)\right]^2 e^{-\eta^2} d\eta \qquad (72)$$

or

$$r(z, t) = r_P + \left(\frac{dv'}{dT'}\right)_D f(t) \frac{2}{\sqrt{\pi}} \int_{\frac{z}{\sqrt{4K(t-t_D)}}}^{\infty} \left[\sqrt{1 - \frac{z^2}{4Kt\eta^2}} - \sqrt{\frac{t_D}{t}}\right] e^{-\eta^2} d\eta + \frac{1}{2}\frac{d^2 v'}{dT'^2} f(t)^2 \frac{2}{\sqrt{\pi}} \int_{\frac{z}{\sqrt{4K(t-t_D)}}}^{\infty} \left[\sqrt{1 - \frac{z^2}{4Kt\eta^2}} - \sqrt{\frac{t_D}{t}}\right]^2 e^{-\eta^2} d\eta. \qquad (73)$$

Both integral terms of (73) may be written in a form containing $Y_n(\alpha,\varkappa)$. That one which is included as a factor of the first derivative reads

$$\frac{2}{\sqrt{\pi}} \int_{\frac{z}{\sqrt{4K(t-t_D)}}}^{\infty} \left[\sqrt{1-\frac{z^2}{4Kt\eta}} - \sqrt{\frac{t_D}{t}}\right] e^{-\eta^2} d\eta$$

$$= Y_{\frac{1}{2}}(\alpha,\varkappa) - \sqrt{\frac{t_D}{t}} \frac{2}{\sqrt{\pi}} \int_{\alpha\varkappa}^{\infty} e^{-\eta^2} d\eta, \quad (74)$$

where $\varkappa = \sqrt{t/(t-t_D)}$ and $\alpha = z/\sqrt{4Kt}$.

The integral that is a factor of the second derivative in (73) reads

$$\frac{2}{\sqrt{\pi}} \int_{\frac{z}{\sqrt{4K(t-t_D)}}}^{\infty} \left[\sqrt{1-\frac{z^2}{4Kt\eta^2}} - \sqrt{\frac{t_D}{t}}\right]^2 e^{-\eta^2} d\eta$$

$$= Y_1(\alpha,\varkappa) - 2\sqrt{\frac{t_D}{t}}\, Y_{\frac{1}{2}}(\alpha,\varkappa)$$

$$+ \frac{t_D}{t} \frac{2}{\sqrt{\pi}} \int_{\alpha\varkappa}^{\infty} e^{-\eta^2} d\eta. \quad (75)$$

In (74) and (75), the terms are arranged according to the power of the variable $\sqrt{t_D/t}$. In each equation the first term is the predominant one. The other terms become by degrees insignificant when $t$ increases beyond $t_D$.

The integral $Y_{\frac{1}{2}}(\alpha,\varkappa)$ in (74) and (75) is wanted in terms of more elementary integrals which may be easily computed. For that purpose, it is advisable to divide it into two parts as follows,

$$Y_{\frac{1}{2}}(\alpha,\varkappa) = Y_{\frac{1}{2}}(\alpha,1) -$$

$$- \frac{2}{\sqrt{\pi}} \int_{\alpha}^{\alpha\varkappa} \sqrt{1-\frac{\alpha^2}{\eta^2}}\, e^{-\eta^2} d\eta. \quad (76)$$

The first part is integrated in Appendix B and is mentioned above in (67). The second part has the magnitude of $(t_D/t)^{\frac{1}{2}}$. It may be estimated by means of any approximate form of integration.

The main integral in (75) is easily integrated in parts. We get the equation:

$$Y_1(\alpha,\varkappa) = \frac{2}{\sqrt{\pi}} \int_{\alpha\varkappa}^{\infty} \left(1-\frac{\alpha^2}{\eta^2}\right) e^{-\eta^2} d\eta$$

$$= (1+2\alpha^2)\frac{2}{\sqrt{\pi}} \int_{\alpha\varkappa}^{\infty} e^{-\eta^2} d\eta -$$

$$- \frac{2}{\sqrt{\pi}} \frac{\alpha}{\varkappa} e^{-\alpha^2\varkappa^2}. \quad (77)$$

Finally, we sum up that when $t \gg t_D$, equation (73) gets the approximate form

$$r(z,t) = r_P + \left(\frac{dv'}{dT'}\right)_D f(t)\, Y_{\frac{1}{2}}(\alpha,1)$$

$$+ \frac{1}{2}\frac{d^2v'}{dT'^2}[f(t)]^2\, Y_1(\alpha,1). \quad (78)$$

In Fig. 15, the curves $PA$ and $PBB'$ show the interrelation between $T'$ and $r$ in the air adjacent to a surface at two different moments of radiative heat loss. The former curve ends at $A$. The latter is related to a lower surface temperature, cuts the saturation curve at $B$ and ends at $B'$. Point $C$ is the point of osculation of the tangent drawn from $P$ and is determined solely by the site of $P$ in relation to the curve of saturation. Point $C$ separates two types of curves exemplified by $PA$ and $PBB'$. When the surface temperature is higher than $T'_C$, the water content is below that of saturation at all levels above the surface and the air is unsaturated. On the other hand, the saturation mixing ratio is exceeded between the points $B$ and $B'$ if the surface temperature is lower than $T'_C$. Hence, between the levels of $B$ and $B'$, fog is found.

It is interesting to find that it is not the dew point that is the critical temperature for supersaturation and fog formation but the temperature $T'_C$. It is well known that dew is formed before radiation fog.

After the fog has begun to form, its top is gradually raised. In contrast to the temperature of the base ($B'$), that of the top ($B$) exceeds $T'_C$

and increases when the surface temperature decreases.

At any stage when the surface temperature still exceeds $T'_C$, the curve $PA$ turns its convex side upwards. The opposite happens when the surface temperature has fallen below $T'_C$. This phenomenon is easily understood to be caused by the variation of $E/H$ in (37) and its lag in the upper part of the transition layer above the surface in relation to the change that is initiated at the surface. It is interesting to note that Taylor mentioned this in his paper of 1917. When the surface temperature falls at $T'_C$, the lowest part of the curve is retained parallel to the tangent at $C$ and $PC$ is almost a straight line. We can approximate $PC$ to the tangent of the saturation curve. If we should use the preceding formula (72) in order to find $T'_C$, the estimation will be very complicated but the result will differ very little from that which assumes $PC$ to be a tangent. The latter assumption gives the following equality between the inclinations of the curve and the tangent at $C$:

$$\left(\frac{dv'}{dT'}\right)_C = \frac{r_P - v'_C}{T'_P - T'_C}. \tag{79}$$

We replace $v'_C$ by its expansion in form of *Taylor's series*,

$$v'_C = v'_P - \left(\frac{dv'}{dT'}\right)_C (T'_P - T'_C) - \frac{1}{2}\frac{d^2 v'}{dT'^2}(T'_P - T'_C)^2$$

and substitute $v'_P + w_P$ for $r_P$. Then we get

$$-w_P = \frac{1}{2}\frac{d^2 v'}{dT'^2}(T'_C - T'_P)^2.$$

For example, $T'_C$ is $+5.9°$C when $T'_P = +10.0°$C and $T_D = +9.5°$C.

In (70) we find another equation for $-w_P$:

$$-w_P = \left(\frac{dv'}{dT'}\right)_P (T'_P - T_D) - \frac{1}{2}\frac{d^2 v'}{dT'^2}(T'_P - T_D)^2.$$

By putting these two in relation to each other, we get

$$\left[\frac{T'_P - T'_C}{T'_P - T_D}\right]^2 = \frac{2}{T'_P - T_D} \cdot \frac{\left(\frac{dv'}{dT'}\right)_{PD}}{\frac{d^2 v'}{dT'^2}}, \tag{80}$$

where $\left(\frac{dv'}{dT'}\right)_{PD} = \frac{1}{2}\left[\left(\frac{dv'}{dT'}\right)_P + \left(\frac{dv'}{dT'}\right)_D\right]$.

We recall the boundary condition

$$T'(0, t) = T'(0, 0) - N'\sqrt{t}.$$

By means of this, we get the time when fog begins to form either in terms of the difference between the wet-bulb temperature and the dew point,

$$t_C = \frac{T'_P - T_D}{(N')^2} \cdot \frac{\left(\frac{dv'}{dT'}\right)_{PD}}{\frac{1}{2}\frac{d^2 v'}{dT'^2}}$$

or, in relation to the spell of cooling of the surface to the dew point,

$$t_C = \frac{\sqrt{t_D}}{N'} \cdot \frac{\left(\frac{dv'}{dT'}\right)_{PD}}{\frac{1}{2}\frac{d^2 v'}{dT'^2}}.$$

Both equations give useful aspects on the problem of fog prediction. The values of the quotient between the first and second derivatives of $v'$ is 12 at $-30°$, 15 at 0° and 18 at $+30°$C. For example, when $T'_P$ is $+10.0°$ and $T_D$ $+9.5°$C, $t_C/t_D$ is about 64. See second stage in Fig. 16 below. That means that if the surface is cooled by radiative heat loss to the dew point in five minutes and the net radiative heat loss is retained, fog begins to form five hours later. The remarkable difference between $t_C$ and $t_D$ is due to our assumption that the temperature depends on the square root of time. If the relation were linear, the quotient of the square of the temperature differences in (80) would be equal to $(t_C/t_D)^2$ instead of $t_C/t_D$. In our example, that change would imply that the fog begins to form about 35 minutes instead of five hours after the dew point is reached.

In Fig. 16, a series of five profiles of radiative fog is shown. For their estimation, the formulae of this section are used. Each of the five stages shown is put along a common horizontal time scale. The unit time interval is $t_D$. Owing to the condition that the temperature change is inversely proportional to the square root of time, the surface temperature changes initially very

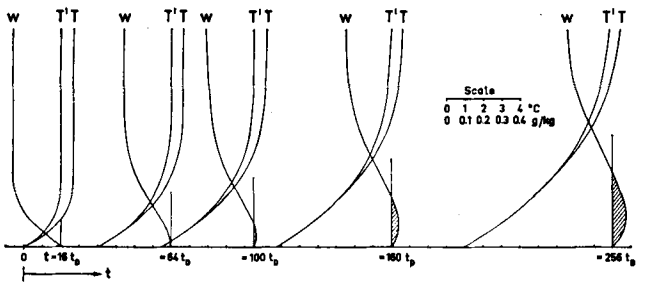


FIG. 16. Profile curves of $T$, $T'$ and $w$ in radiation fog computed by means of (58) and (59). The unit of the time scale is the spell of fall of surface temperature to the dew point from the commencement of radiative cooling.

rapidly and $t_D$ is a relatively short spell. Fog begins to form when the lowest part of the $w$ profile shifts to the right of the vertical line indicating $w = 0$. After that, the height of the fog increases.

It is worth while to compare Figs. 13 and 16, which deal with radiation fog and advection fog, respectively. In both cases, the depth of the temperature transition layer and the height of the fog increase, but in advection fog the height of fog is retained in a constant part of the transition layer. In radiation fog, on the other hand, the relative height of fog within the transition layer increases owing to the decrease of the temperature at the base ($B'$) and the rise of the temperature at the top ($B$).

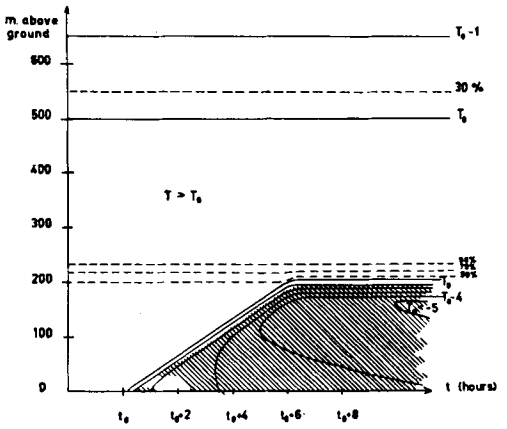


FIG. 17. "Schematic time cross section showing the variation in temperature and relative humidity on the formation of fog under late autumn and winter conditions in an undisturbed weather situation. Solid lines represent temperature in °C, dashed lines relative humidity in per cent and hatched areas fog or Stratus. The effective net radiation is assumed to start at time $t_0$, the relative humidity to remain above 90 % up to 200 m and decrease rapidly subsequently to below 50 %, and the wind velocity to be weak up to at least 400 m. The highest relative humidity (about 100 %) is found in the transition layer." Figure and legend from MORALES (1958).

## 11. The effect of the black-body emissivity of drops on radiation fog

A time cross section that gives some features of radiation fog is reprinted in Fig. 17 from a paper of MORALES (1958). The cross section is based on measurements by means of radiosoundings with a tethered balloon. Morales points out three essential conditions that must be present if any substantial amount of fog is to be formed:

1. Effective net upward radiative heat flux.
2. Light gradient wind.
3. High relative humidity not only next to the ground but also at heights of 100 m or more.

Before the fog is formed, the ground is cooled by the net upward flux of long-wave radiation. A temperature inversion of such a magnitude is established adjacent to the ground that the eddy transfer of heat content balances the radiative heat loss. If the humidity of the air is high, fog is formed in the temperature inversion as described in the previous section. The higher the humidity of the air the greater is the maximum of water-drop mixing ratio in the fog. In consequence, the upper part of the fog layer partly or completely takes over the role of radiating surface initially played by the ground surface. In that way, a temperature transition layer is formed at the top of the fog and the surface inversion disappears.

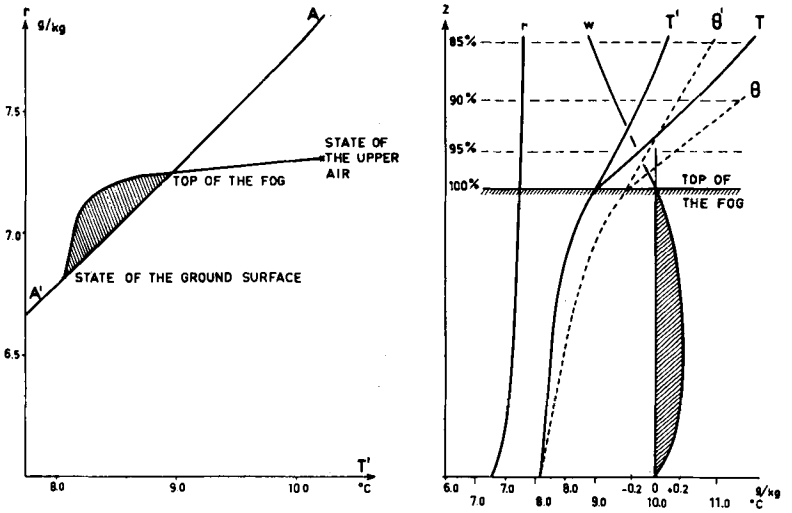


FIG. 18. *Left:* The interrelation between $T'$ and $r$ in radiation fog and in warm-air advection fog of which the upper part is subject to radiative heat loss. *Right:* The profiles of $w$, $T$, $T'$, and $r$ relate to the diagram on the left. The horizontal, dashed lines show the vertical variation of relative humidity above the fog.

In the following discussion, which aims at pointing out the fundamental reason for some of the fog characteristics described by Morales, we retain our basic assumption which we viewed in Section 9 in the light of a paper of IMAHORI (1953). That assumption is that the content of vapour plus drops is transferred by turbulence in just the same way as any other conservative property of the air. The assumption implies that no water drops fall out by coalescence and no precipitation occurs. As a matter of fact, the assumption is never completely fulfilled in natural conditions. But somewhere between two extreme situations, the truth should be found, and we put the question which of these extreme limits is generally approached in reality. The two extreme situations are, first, complete turbulent exchange of drops in fog and, secondly, complete resistance of the drops to eddy motions. It seems to the present author that the applicability of his hypothesis to observed facts is in favour of the former alternative.

On the basis of our assumption, we have represented the interrelation between the temperature and the water content by means of an integral curve of (37) in the $T',r$ diagram. The inclination of the curve to the abscissa depends on the quotient $E/H$, i.e. the ratio of eddy transfer of total water content to the eddy transfer of total heat content.

Morales verified that the radiation fog is formed between the ground and an upper stratum of maximum specific humidity at 100–300 m or more. In the intermediate layer, an eddy transfer of water content is maintained down to the surface.

In the right-hand part of Fig. 18, a profile of the distribution of total content of water is drawn. It is slightly curved because of the upward increase of the coefficient of eddy exchange. Under the condition mentioned above, the net transfer of total water content is not affected by the presence of fog. In stationary conditions, it is constant between the "sink" at the ground and the "source" at the level of maximum specific humidity. On the other hand, the eddy transfer of total heat content balances the radiative net flux established by the emissivity of the drops. The net radiative flux is directed upwards and is constant above the top but decreases downwards from the top. In consequence, the eddy heat transfer, which is directed downwards, is constant above the top but decreases, too, in the fog downwards and the temperature profile $T'$ in the right-hand part of the figure has a convex form in the fog layer. We mentioned that, in the $T',r$ diagram, the inclination of the integral curve showing the interrelation between $T'$ and $r$ depends on the quotient of the transfer of total water content

and the transfer of total heat content, $E/H$. As shown by Morales—more clearly in his individual cross sections than in Fig. 17—the gradient of specific humidity is not significantly great above the top of the fog. That means that the eddy transfer of total water content seems not to exceed normal conditions to any noteworthy extent. On the other hand, the radiative heat loss might be expected to be relatively great since it is one of the particular conditions of fog formation. In consequence, the eddy transfer of heat content is much greater than normal above the top of the fog and the inclination of the integral curve to the abscissa is significantly small to the right of the curve of saturation. Downwards from the top of the fog, the eddy transfer of heat content decreases according to the decrease of the net radiative heat flux. But the eddy transfer of water content is retained constant throughout the fog layer. That is the reason why the inclination of the integral curve to the left of the saturation curve in the $T',r$ diagram increases downwards. At the temperature of the ground surface—only a few degrees Centigrade from the temperature of the top—the integral curve ends at a point on the curve of saturation mixing ratio. There, its inclination to the abscissa is maximum. The hatched area enclosed by the two curves represents the liquid-water content of the fog. The hatched area enclosed by the $w$ profile in the right-hand part of the figure gives another representation of the vertical distribution of liquid-water surplus.

Owing to the great convex curvature of the integral curve in the $T',r$ diagram, the magnitude of liquid-water content in fog may be relatively great; the temperature difference between the top and the base of the fog is smaller than we supposed in the preceding sections to be required for a substantial formation of fog.

Here, we should interpose the remark that such a height of the fog layer as is described by Morales in Fig. 17 does not permit us to disregard the vertical pressure variation, i.e. our assumption (ii) in Section 7 fails. The potential wet-bulb temperature $\theta'$ should be retained in formula (32) and substituted for $T'$ in the differential equation of (40). Then, a temperature profile that satisfies (40) in terms of the potential wet-bulb temperature is one of the first concepts that we get at an integration across the fog layer. It is drawn in the right-hand part of Fig. 18 as a dotted profile curve. In the next step of the computation, we estimate the "real" wet-bulb temperature by means of formula (31). After integration of the differential equation (41), which is not subject to any transformation on account of the pressure gradient, we get the profile of total water content and, finally, the interrelation between wet-bulb temperature and total water content in the $T',r$ diagram.

We need not go into further details if we want only a rough estimation of the effect of the pressure gradient. We see that the vertical increase of the potential temperature in Fig. 18 is greater than that of the real temperature. This implies that the downward eddy transfer of heat content even in the fog is greater than we at first assumed. A vertical lapse of the air temperature is possible through additional increase of radiative heat loss at the top of the fog and would result in a further increase of the shaded area in the $T',r$ diagram showing the liquid-water content.

The consideration of the vertical pressure variation does not change any basic idea of the present theory of fog formation but only modifies the quantitative estimation. Since we have no experimental data that permit us to undertake a detailed verification, we are less interested in exact quantitative estimations than in finding simple theoretical aspects and pointing out the factors that are vital to fog formation. In consequence, we shall continue in what follows to disregard the effect of the vertical pressure gradient, but shall bear well in mind that we are not allowed to do so when taking the theory as a basis for quantitative computation.

The principal aim of the present section has been to point out the important role played by the water drops in the increase of the fog density. We know from the preceding sections that a relatively strong temperature inversion is demanded adjacent to the surface for the initial formation of fog. In Fig. 18, we have learnt that at a later stage, when the radiative emissivity of the drops is effective, a much smaller temperature difference between the base and the top of the fog is needed in order to keep a considerable amount of water-drop density. It seems that the drops of fog, by virtue of their radiative emissivity, themselves produce one of the most vital conditions for their own existence.

Above the top of the fog, negative values of $w$ in Fig. 18 relate to unsaturated air. There is an upward decrease of relative humidity as shown by the dashed horizontal lines. A discontinuity of the gradient of the dry-bulb temperature is found at the top, but the wet-bulb temperature varies continually. In Fig. 17, Morales placed the temperature inversion mainly in the upper part of the fog; but in fact it probably extends considerably above that into the layer of unsaturated air. It is possible that his humidity measurements did not clearly indicate the top of the fog. The feature described here is, however, evident from other measurements, for example those of URFER (1956). His measurements show that the maximum vertical increase of the temperature is found immediately above the top of the fog, exactly in conformity with the pattern of Fig. 18.

Finally, let us sum up in the light of our theory the conditions that morales found "should be fulfilled if a radiation fog of any importance is to be formed". We note the conditions in his own wording:

1. "*Sufficient effective radiation.*"—At first, the radiative heat loss brings about a strong inversion adjacent to the ground and the fog begins to form there. In the "mature" state of the fog, the radiation maintains the important convex bend of the integral curve in the $T',r$ diagram.

2. "*Light gradient winds.*"—A slight amount of turbulence in the surface boundary layer is found even with calm or light gradient winds. The light gradient wind may cause an advective flow which at the top of the boundary layer maintains a supply of heat content and vapour. The form of the integral curve of (37) in the $T',r$ diagram does not depend on the magnitude of turbulence, since (35) does not contain the absolute value of the coefficient of eddy exchange but the quotient of $K_E/K_H$. In (37), the latter is approximated to unity. On the other hand, in his statement of the condition Morales implies that the gradient wind should not be too strong. If the wind is strong, the coefficient of eddy exchange may be so great that the advection of vapour is insufficient to maintain such a high water content in the air as is demanded by the condition stated in the next paragraph.

3. "*High relative humidity, not only in the air strata nearest to the ground but also at a height of 100 metres or more.*"—In terms of our theory, the condition means that the air at the top of the surface boundary layer should fix a point in the $T',r$ diagram as close as possible to the saturation curve. For upward growth of fog it is necessary for this condition to be fulfilled not only when the first fog is formed adjacent to the ground but also when the height of the fog has increased to 100 m or more.

## 12. The effect of the selective emissivity of vapour and carbon dioxide

It might be asked whether any kind of radiative emissivity other than the black-body emissivity of the drops could have the effect on fog formation described above. In Section 3, the cooling effect of the radiative emissivity of moist air was considered in the light of an idea that was put forward by EMMONS & MONTGOMMERY in 1947. We arrived at the conclusion that the effect in question could not itself produce fog, since we also have to take into consideration the eddy exchange. We shall now review the idea once more, but this time in the light of the preceding section.

By means of (37), we find the inclination of the integral curve in the $T',r$ diagram:

$$tg\,\alpha = \text{const}\,\frac{dr}{dT'} = \text{const}\,\frac{E}{H}\left[c_p + T'\frac{d}{dT'}\left(\frac{Lv'}{T'}\right)\right]. \qquad (81)$$

The constant depends on the scales of the ordinate and the abscissa in the $T',r$ diagram.

If there is any time variation in the quotient $E/H$, the inclination will of course vary accordingly. We have learnt about this in Section 10, where the formation of radiation fog was discussed. In what follows, we shall assume that steady conditions prevail, so that the quotient of $E/H$ does not depend on time but only on vertical variations. In accordance with the preceding section, we shall also assume that the eddy transfer of water content is constant between the top and the base of the boundary layer but that the eddy transfer of heat content responds to the variations of radiative heat flux within the layer.

By logarithmic differentiation of (81) and by multiplication by $\cos\alpha$ we get the curvature of the integral curve (37) in terms of the variations of eddy transfer of heat:

$$\cos\alpha\frac{d\alpha}{dT'}=G\left[1-\frac{1}{G}\frac{1}{H}\frac{dH}{dT'}\right]\sin\alpha\cos^2\alpha. \quad (82)$$

We recall that the description of the logarithmic derivative $G$ is found in (42) and in Fig. 10. When the eddy transfer of heat content is constant along the vertical, $dH=0$. The curvature is then settled by $G$ only and is positive. Hence, when the integral curve is not affected by variations of $H$, it turns its convex side down as shown by $BB'$ in Fig. 5. The condition for the curve having a convex bend as shown in Fig. 18, is that

$$\frac{1}{H}\frac{dH}{dT'}>G.$$

We note some values of $G$:

| | |
|---|---|
| At $-30$°C: | $G=0.006$°C$^{-1}$ |
| $\pm0$ | 0.025 |
| $+30$ | 0.040 |

In what follows we shall refer to two papers which deal with measurements of heat balance in the boundary layer immediately above the ground surface. First, RIDER & ROBINSON (1951) made a large number of measurements above a surface of short grass in lapse as well as inversion conditions. Secondly, KRAUS (1958) investigated the heat balance in radiation fog in an area of clean-cut wood, where the average height of grass and young pine trees was 40 cm. On one occasion the observations by the first-mentioned authors cover a spell of radiation fog formation. Kraus succeeded once in recording a radiation fog from the beginning to the end during six and a half hours.

At present, we are interested in observations of the vertical change of the radiative heat flux. Neither Rider & Robinson nor Kraus measured this, but they computed it by means of either the *Elsasser chart*, the *Kew chart* described by ROBINSON (1950), the numerical method of BRUINENBERG (1946), or the tabular method of BROOKS (1950). It should be mentioned that Kraus tried to measure the vertical change of radiative heat flux in fog but failed. He made a rough estimation of the radiative effect of drops and added this to the effect of vapour and carbon dioxide.

Of course, the conditions of steady state are not fulfilled in field investigations. Then, the components of heat balance are not only the eddy heat transfer and the radiative heat flux but also the heating or cooling of the air.

Equation (82), however, refers to steady conditions. We replace the derivative in the right-hand member by a quotient of the finite differences $\Delta H$ and $\Delta T'$ and put for $-\Delta H$ the above-mentioned estimations of the vertical change of radiative heat flux. For $H$, we retain the data of eddy transfer of total heat content. Then, we get by means of (82) the curvature attributed to the integral of (37) in conceived steady cases which are fixed by observed values of these three concepts.

The notations of the concepts in question are as follows in the papers of Rider & Robinson and Kraus:

| Ours | Rider & Robinson | Kraus |
|---|---|---|
| $-\Delta H$ | $R(100)-R(0)$ | $-(S-S_{z_0})$ |
| $H$ | $C(0)+\lambda E(0)$ | $-(L+V)$ in clear air<br>$-\varphi(T')L$ in fog. |

The coefficient $\varphi(T')$ is ours and reads

$$\left[1+\frac{T'}{c_p}\frac{d}{dT'}\left(\frac{Lv'}{T'}\right)\right].$$

In fog, $(L+V)$ is not identical with the total heat transferred since Kraus does not take into consideration the effect of latent heat. Our correction is based on (32) and the fact that Kraus' $L$ is equivalent to $+\varrho c_p K(\partial T/\partial z)$.

In Fig. 19, we find the values that are computed by means of the data given by RIDER & ROBINSON (1951) for the approximate bracket term in (82),

$$1-\frac{1}{G}\frac{1}{H}\frac{\Delta H}{\Delta T}.$$

Each dot refers to an observation usually covering a spell of 30 minutes. The investigation is confined to the lowest metre of the air layer above the surface. We find that the values depend closely on the temperature difference between the top and the base of the layer. In

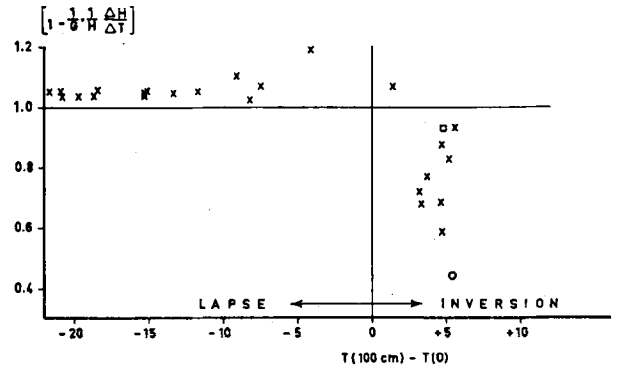


FIG. 19. The bracket term $\left[1-\frac{1}{G}\frac{1}{H}\frac{\Delta H}{\Delta T}\right]$ in equation (82) as a function of the temperature difference $\Delta T$ in a surface boundary layer. The depth of the layer is 100 cm. Each dot refers to thirty minutes' observations published by RIDER & ROBINSON (1951). □ Fog began to form just as the observations were finished. ○ Fog formed during the run of the observations.

lapse conditions, i.e. when the surface is heated by solar radiation, the values slightly exceed unity and are almost constant. In inversion conditions, i.e. when the surface is cooled by long-wave radiative outflow, the values are smaller than in lapse conditions and are dispersed between $+1.0$ and $\pm 0$. In these cases, fog occurred twice. On November 26, 1948 (marked □) radiation fog began to form at 1750 hr just when the measurement had finished. At 1805 hr, the top of the fog was above two metres. On September 10, 1949 (marked ○) the observation lasted from 2113 hr to 2143 hr and fog was first observed at 2125 hr and "drifted slowly in patches during the remainder of the observation" (*ibid.*). It is noteworthy that this case is represented by an extreme point in Fig. 19. In consequence, the integral curve (37) in the $T',r$ diagram approaches the form of a straight line in this case more than in any other in Fig. 19. The area between the integral curve and the saturation curve is accordingly increased, which argues in favour of a reasonable content of liquid water in the fog.

In Fig. 20 is represented the variation that

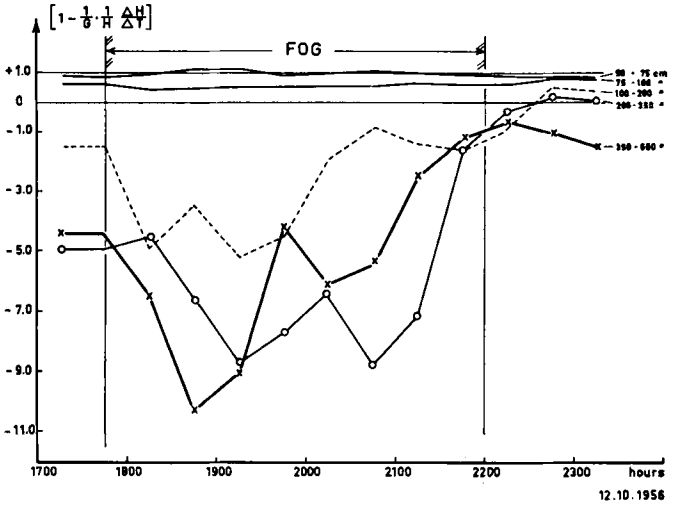


FIG. 20. The variation of the bracket term $\left[1-\frac{1}{G}\frac{1}{H}\frac{\Delta H}{\Delta T}\right]$ in equation (82) during a spell of fog. The values are computed with the use of data published by KRAUS (1958). The fog lasted from 1735 hr to 2200 hr. The depth of the fog was constantly about 200 cm. The curves refer to five sublayers between 50 and 600 cm.

we get for the above-mentioned approximate bracket term in (82) on the occasion of radiation fog described by Kraus. He performed his observations on the layer extending up to six metres above the surface and he divided the layer into five sublayers. Each of the sublayer is represented by a curve which is somewhat smoothed by putting mean values of two successive observations along the abscissa at points a quarter past each observation at half and full hours. The first patches of fog were observed by Kraus at 1735 hr. At 1745 hr the fog was very dense and its depth was two metres. During the rest of its existence, the fog retained its top at that height. The fog dissipated at 2200 hr on an increase of wind.

We see from the figure that the two sublayers within 1 m above the surface occupy an exceptional position. There, the curves do not pass below zero, so that the value of the bracket term in (82) lies between $+1.0$ and $\pm 0$, exactly as is found in inversion conditions in Fig. 19. Indeed, the dots in Fig. 19 refer to the same levels above the surface as the two upper curves in Fig. 20. There is one more point of agreement in these levels between the two diagrams. In both cases a slight minimum is found during fog.

The next curve in Fig. 20 refers to the sublayer at 100–200 cm and according to Kraus it represents the top layer of the fog. It indicates negative values, and there is a significant minimum during the first part of the existence of fog. Further, there are two curves in the diagram, each representing a sublayer above the fog. On average, the sublayer (200–350 cm) immediately above the fog has the greatest negative values. But sometimes, the negative values in that layer are exceeded by those in the highest layer considered (350–600 cm).

It seems a little confusing that the maximum negative values are not found in the sublayer immediately below the top of the fog but at some metres above it and that the curve marked 350–600 cm still indicates relatively great negative values. Probably, however, we are not justified in drawing such detailed conclusions from the data of Kraus' investigation. The variation of (82) depends chiefly on the quotient of $\Delta H$ and $\Delta T$. The latter term is currently measured during the evening in question, but the former is based on only one estimation of the vertical change of the radiative heat flux in fog. There is such an obvious difference between the qualities of these two terms that we should beware of drawing too detailed conclusions from Fig. 20. This warning especially concerns any detailed comparison of features within the spell of fog.

More significant may be differences between any two features in Fig. 20 before and after the dissipation of the fog, respectively. Thus, the figure shows a significant rise of the curves from the conditions of fog to those of clear air. When the fog has disappeared the bracket term in (82) is of the same order of magnitude in almost all the layers considered. This proves our theory that the conditions of fog greatly affect the curvature of the integral curve in the $T',r$ diagram and make it more convex in conditions of fog than in those of clear air.

We conclude that a vertical variation of eddy transfer of heat content is probably brought about most effectively in the top layer of the fog. FLEAGLE, PARROT & BARAD (1952) discuss this item theoretically as well as experimentally. They show that in two or three hours the long-wave radiative cooling of the fog top at about 200 feet may radically change a very stable temperature profile in the fog into one of neutral stability. At the top, the inversion originally found at the ground is simultaneously re-established. The authors also show that at the top of the fog the radiative heat loss is correlated to a discontinuity of eddy heat transfer. They prove the condition that if there is a too great eddy transfer of heat in the inversion above the fog in relation to the radiative heat loss the neutral stability will not be reached in the fog, but a slight inversion is retained there.

## 13. The effect of the black-body emissivity of drops on advection fog

In the three preceding sections, the discussion has dealt with radiation fog. Before that we also discussed the principal pattern of "pure" advection fog, which is not affected by radiation. We shall now, in the light of the last three sections, review the formation of advection fog and pay regard to the effect of the black-body emissivity of the drops. The latter factor is expected to be important since it is well known that many cases of fog may be classified as "mixed" types of radiation and advection fog.

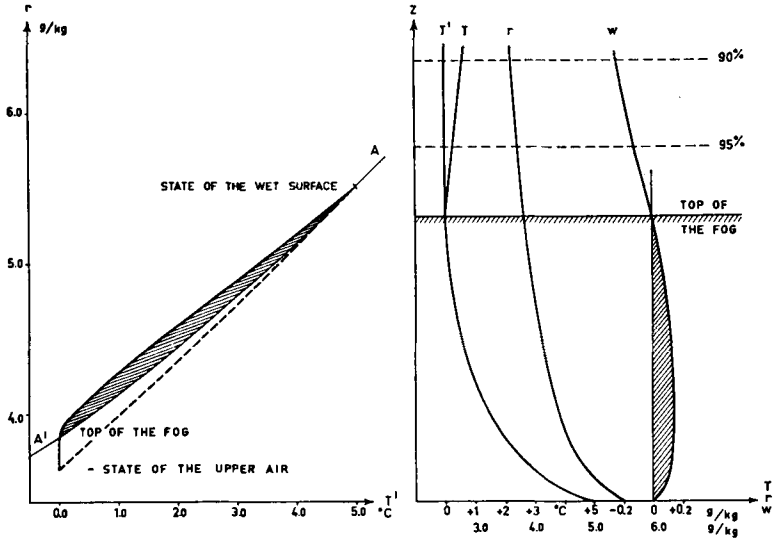


FIG. 21. *Left:* The integral curve of (37) in cold-air advection fog that is subject to radiative heat loss in its upper part. *Right:* The profiles of $w$, $T$, $T'$ and $r$ in cold-air advection fog relating to the diagram on the left. The relative humidity distribution in the unsaturated air is indicated by the horizontal dashed lines.

We shall take separately the cases of cold air and warm air. We start with *warm-air advection fog* and refer to the illustration of its characteristics in Fig. 18. The temperature decreases downwards from the upper stratum of unmodified air to the cold surface of the ground. In order to balance the radiative outflow at the fog top, the downward transfer of heat must be greater above the fog than in it. In a steady state this condition responds to a greater gradient of wet-bulb temperature above the top of the fog than below it.

On the other hand, the eddy transfer of total water content is not affected by the fog and is, in a steady state, independent of height. The vertical variation of the eddy heat transfer causes the inclination of the integral curve in the left-hand part of Fig. 18 to increase downwards from the top of the fog and to reach a maximum at the ground surface.

The features of "mixed" warm-air advection fog are identical with those of radiation fog in non-advective conditions.

The essential difference between "pure" and "mixed" advection fog is found in the temperature difference between the top and the base of the fog. The difference is much less in "mixed" than in "pure" advection fog.

In the case of *cold-air advection fog*, the unmodified air in the upper stratum is colder than the ground surface, as shown in Fig. 21. Owing to the radiative heat loss at the top of the fog, an upward eddy transfer of heat is maintained below the top but is almost eliminated above. In consequence, the temperature gradient is very small above the fog but considerably greater in it. In the figure, the example of zero wet-bulb temperature gradient above the top is chosen. That means that the net radiative heat flux completely replaces the eddy transfer of total heat content. But there is a slight inversion in the dry-bulb temperature gradient. This indicates a downward transfer of sensible heat which balances the upward transfer of latent heat. The eddy transfer of total water content is not affected by the fog. Indeed, the present theory demands that there shall be evaporation at the surface in spite of the presence of fog, because the gradient of total water content differs from zero. Thus, there are vertical variations of the quotient $E/H$ due only to variations of the eddy transfer of total heat content. In the $T'$,$r$ diagram, the inclination of the curve of interrelation between $T'$ and $r$ is related to that quotient. In Fig. 21, the curve is vertical below the saturation curve

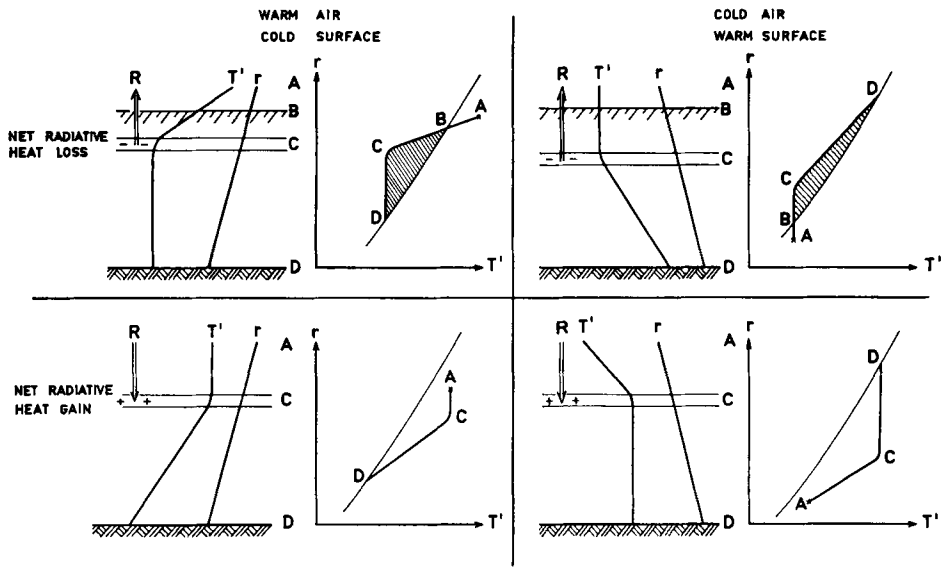


FIG. 22. Comparison of the effects of radiative heat loss and heat gain on fog. *Upper part:* Net radiative heat loss. *Lower part:* Net radiative heat gain. *Left:* Warm air adjacent to a cold surface. *Right:* Cold air adjacent to a warm surface.

but turns sharply to the right there above where $H$ decreases downwards in the fog. It ends on the saturation curve at the temperature of the base of the fog. The area enclosed by the two curves represents the liquid-water content of the fog. That representation is also given by the shaded area in the $w$ profile in the right-hand part of the figure.

To sum up, "mixed" advection fog extends vertically over a considerably smaller temperature interval than "pure" advection fog. The dashed line in the $T',r$ diagram in Fig. 21 is the integral curve of (37) drawn with constant quotient $E/H$ between the wet surface and the unmodified air. Along this dashed line, interrelated values of $T'$ and $r$ would be found if no radiation effect were displayed. We observe that it does not intersect the saturation curve. Extreme vertical temperature differences are conditional for fog formation in "purely" advective conditions.

## 14. Conclusions

In Sections 8 to 10, the author presented the most elementary form of the interrelation between the temperature and the total water content in a boundary layer adjacent to the ground surface. The interrelation is represented by an integral of (37) with the appropriate boundary conditions. In non-radiative, steady conditions, the coefficient $E/H$ is constant, and the explicit formula (39) of liquid-water content shows that a great temperature difference across the transition layer is required for an appreciable amount of liquid water to be formed. Indeed, the temperature difference in question seems to be very large in comparison with generally prevailing conditions in fog.

On the other hand, the examples of Figs. 18 and 21 show that, *at a much smaller temperature difference across the fog layer, a reasonable content of liquid water is established if the sink of eddy heat transfer is not located at the same level as that of eddy water transfer.*

In Fig. 22, further light is thrown on this matter by means of a schematic comparison of four diametrically different cases. The two at the top relate to the situation where a sink of eddy heat transfer responds to radiative heat loss within the fog, here concentrated in a narrow zone at $C$. Then, the major part of the eddy heat transfer is found *above* the fog and is directed downwards in the case of warm air (left-hand part of the figure) but is found *within* the fog and is directed upwards in the case of cold air (right-hand part). The result is in both

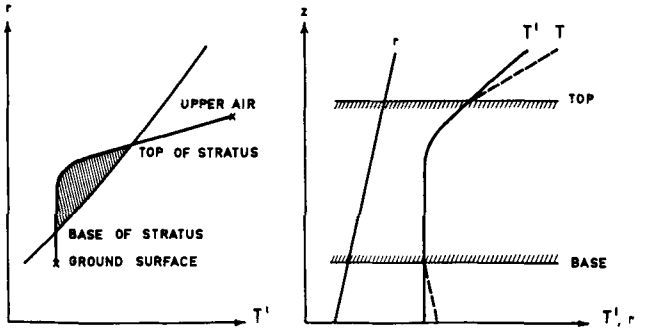


FIG. 23. The distribution of temperature and water content in a layer of low Stratus and its representation in the $T',r$ diagram.

cases that a discontinuity of the gradient of the integral curve of (37) is established at $C$ such that the area $DCBD$, which represents the liquid-water content, is relatively large.

It is easy to imagine the pattern in the $T',r$ diagram that would result if instead of a net loss of radiative heat there were an accumulation of it or, in other words, if there were a source of eddy heat transfer within the fog. The lower parts of Fig. 22 show such cases. The curve $ACD$ assumes such a trend that it will not cut the saturation curve at all except that it ends on the curve if the surface is wet. Thus, a gain of radiative heat cannot prevail in a steady fog, for it will tend to dissipate the fog. This indeed is a well-known fact; but it is here brought into consideration from a new point of view.

Finally, attention is drawn to the advantage of applying the present theory and the $T',r$ diagram for the understanding of any kind of fog formation or transformation. Two examples are here touched upon:

*The transformation of warm-air advection fog into Stratus* (Fig. 23). We assume that the fog is advected to a dry surface. This implies that the surface boundary condition, which originally is fixed to a point on the saturation curve in the $T',r$ diagram, is moved to some point below the curve, as shown in Fig. 23. The integral curve of (37) extends across the saturation curve at its two ends and the lower intersection between the two curves represents the base of the Stratus. Since there is still a vertical gradient of water content above the dry surface we cannot deprive the dry surface of its ability to absorb water as we did in Section 10.

*Fog formation by industrial smoke* (Fig. 24). If industrial smoke forms an extended turbid layer below a temperature inversion, it has the same radiative effect as the top layer of fog. Thus, the smoke forms a level of radiative heat loss and establishes the above-mentioned very important difference between the height of the sink of eddy heat transfer and that of the sink of eddy water transfer. The latter is still found at the surface but the former is at the level of the smoke. The convex bend of the integral curve of (37) is now not necessarily fixed to

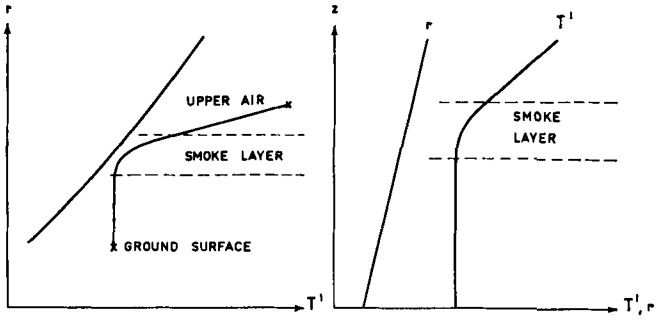


FIG. 24. The distribution of wet-bulb temperature and humidity in a temperature inversion formed by industrial smoke.

the area of saturated conditions above the saturation curve but might also lie in the part of the $T', r$ diagram that represents unsaturated conditions, see Fig. 24. Owing to the bend, however, there is a greater approach to saturated conditions in the turbid layer than in the air above and below it. If cooling occurs, which might happen either because of advection over a cold surface or because of increased radiative heat loss in the turbid layer, saturation conditions are first reached at the turbid layer and later also in the air below that layer. Thus, Stratus is formed in the layer of industrial smoke and the base of the cloud is successively lowered. Finally, when the temperature of the surface reaches the dew point, fog is attained.

To sum up, industrial smoke seems to form Stratus and fog not only because of a hygroscopic property but also because of the blackbody long-wave emissivity of the particles.

## Acknowledgements

Many of the preceding ideas originate from particular problems that I have met in the course of my duties at the Swedish Meteorological and Hydrological Institute. I am much indebted to Dr. Alf Nyberg, the Director of the Institute, for giving me the opportunity to present them in this generalized form.

I wish to thank Professor Gösta H. Liljequist, of the University of Uppsala, for his kind interest in my work.

I appreciate very much the valuable discussions with Mr. Christer Morales on the topic of fog.

Thanks are also due to Mr. Richard Cox, who has put my original wording into correct English, Mrs. Elinor Rapp, who has very kindly drawn the figures, and Mrs. Inger Bonsdorff, who has done a good deal of the typewriting.

## Appendix A

List of Symbols

| | |
|---|---|
| $B$ | *Bowen ratio* |
| $c$ | Specific heat of liquid water |
| $c'$ | Specific heat of saturated vapour |
| $c_p$ | Specific heat of dry air at constant pressure |
| $c_p'$ | Specific heat of unsaturated vapour at constant pressure |
| $E$ | Eddy transfer of total water content |
| $f(t)$ | $\equiv -N'\sqrt{t}$ |
| $G$ | A logarithmic temperature derivative of specific heat of saturated air, see (42) |
| $H$ | Eddy transfer of total heat content |
| $\mathbf{H}$ | Total heat content |
| $K$ | Coefficient of eddy exchange |
| $k$ | *von Karman's constant* |
| $L$ | Latent heat of evaporation |
| $N$ | A constant in (60) |
| $N'$ | The constant in (60) when the equation is referred to the wet-bulb temperature. The relation between $N$ and $N'$ is given in (63). |
| $p$ | Atmospheric pressure of dry air |
| $q$ | Any small quantity of sensible heat |
| $R$ | Gas constant for dry air |
| $r$ | Mixing ratio of total water content |
| $\mathbf{S}$ | Entropy |
| $T$ | Dry-bulb temperature of the air |
| $T'$ | Wet-bulb temperature of the air |
| $t$ | Time co-ordinate |
| $u$ | Wind velocity in the direction of the $x$-axis |
| $u_*$ | Frictional velocity |
| $v$ | Saturation mixing ratio of vapour |
| $v'$ | Saturation mixing ratio of vapour at the wet-bulb temperature |
| $w$ | Mixing ratio of liquid-water content |
| $x, y$ | Horizontal co-ordinates |
| $Y_n(\alpha, \varkappa)$ | See equation (66) |
| $z$ | Vertical co-ordinate |
| $z_0$ | Roughness parameter |
| $\alpha$ | See equations (66) and (81) |
| $\beta$ | A coefficient in the wind profile equation (56) |
| $\gamma$ | A coefficient in the temperature profile equation (1) |
| $\theta$ | Potential dry-bulb temperature |
| $\theta'$ | Potential wet-bulb temperature |
| $\varkappa$ | See equation (66) |
| $\varrho$ | Density of dry air |
| $\phi$ | See equation (52) |

## Appendix B

INTEGRATION OF $Y_{\frac{1}{2}}(\alpha,1)=\frac{2}{\sqrt{\pi}}\int_{\alpha}^{\infty}\sqrt{1-\frac{\alpha^2}{\eta^2}}e^{-\eta^2}d\eta.$

The integral $Y_{\frac{1}{2}}(\alpha,1)$ is found in some of the formulae of Section 10 relating to radiation fog formation. In what follows, we shall simply call the integral $Y$. In order to get to the final integral form, we first differentiate $Y$ with reference to variations of $\alpha$,

$$\frac{dY}{d\alpha}=-\frac{2}{\sqrt{\pi}}\left[\sqrt{1-\frac{\alpha^2}{\eta^2}}\cdot e^{-\eta^2}\right]_{\eta=\alpha}-\frac{2}{\sqrt{\pi}}\int_{\alpha}^{\infty}\frac{\alpha}{\eta^2}\frac{1}{\sqrt{1-\frac{\alpha^2}{\eta^2}}}e^{-\eta^2}d\eta.$$

The first term is zero. The second is easily integrated in parts,

$$\frac{dY}{d\alpha}=-\frac{2}{\sqrt{\pi}}\left[\sqrt{1-\frac{\alpha^2}{\eta^2}}\frac{\eta}{\alpha}e^{-\eta^2}\right]_{\alpha}^{\infty}+\frac{1}{\alpha}\cdot\frac{2}{\sqrt{\pi}}\int_{\alpha}^{\infty}(1-2\eta^2)\sqrt{1-\frac{\alpha^2}{\eta^2}}e^{-\eta^2}d\eta.$$

The first term is zero. The remainder reads

$$\frac{dY}{d\alpha}=\frac{1}{\alpha}\cdot Y-\frac{2}{\alpha}\cdot\frac{2}{\sqrt{\pi}}\int_{\alpha}^{\infty}\eta\sqrt{\eta^2-\alpha^2}\,e^{-\eta^2}d\eta$$

or

$$\frac{d}{d\alpha}\left(\frac{Y}{\alpha}\right)=-\frac{1}{\alpha^2}\cdot\frac{2}{\sqrt{\pi}}\int_{\alpha}^{\infty}\sqrt{\eta^2-\alpha^2}\,e^{-\eta^2}d(\eta^2).$$

By substitution of $\zeta^2$ for $\eta^2-\alpha^2$, we get

$$\frac{d}{d\alpha}\left(\frac{Y}{\alpha}\right)=-\frac{1}{\alpha^2}e^{-\alpha^2}\cdot\frac{2}{\sqrt{\pi}}\int_{0}^{\infty}2\zeta^2e^{-\zeta^2}d\zeta$$

and may integrate the right-hand member in parts as follows:

$$\frac{d}{d\alpha}\left(\frac{Y}{\alpha}\right)=\frac{1}{\alpha^2}e^{-\alpha^2}\cdot\frac{2}{\sqrt{\pi}}[\zeta e^{-\zeta^2}]_0^{\infty}-\frac{1}{\alpha^2}e^{-\alpha^2}\cdot\frac{2}{\sqrt{\pi}}\int_{0}^{\infty}e^{-\zeta^2}d\zeta$$

$$=-\frac{1}{\alpha^2}e^{-\alpha^2}.$$

The next step of integration gives

$$Y=-\alpha\int_{\alpha}^{\infty}\frac{1}{\eta^2}e^{-\eta^2}d\eta$$

$$=e^{-\alpha^2}-\alpha\left[2\int_{\alpha}^{\infty}e^{-\eta^2}d\eta+C\right].$$

$C$ is the constant of integration and is fixed by the particular form of $Y$ that is presented in the heading of this Appendix. Since $Y$ is a sum of positive terms only it, too, is positive. Further, $0\leqslant\alpha/\eta\leqslant 1$ in the whole interval of integration.

For these two reasons,

$$0<Y<\frac{2}{\sqrt{\pi}}\int_{\alpha}^{\infty}e^{-\eta^2}d\eta$$

and

$$\lim_{\alpha\to\infty}Y=0.$$

Because $Y$ remains finite when $\alpha$ becomes infinite, the constant $C$ of integration must be zero. Hence, the result of our integration is that

$$Y_{\frac{1}{2}}(\alpha,1)=e^{-\alpha^2}-2\alpha\int_{\alpha}^{\infty}e^{-\eta^2}d\eta.$$

## REFERENCES


BEZOLD, W. VON, 1890, Zur Thermodynamik der Atmosphäre. *Sitzber. kgl. preuss. Akad. Wiss. Berlin*, **19**.

BROOKS, D. L., 1950, A tabular method for the computation of temperature changes by infrared radiation in the free atmosphere. *J. Meteor.*, **7**, pp. 313–321.

BRUINENBERG, A., 1946, A numerical method for the calculation of temperature changes by radiation in the free atmosphere. *K. Ned. Meteor. Inst. Meded. Verh., B*, **1**.

BRUNT, D., 1935, Condensation by mixing. *Quart. J. R. Met. Soc.*, **61**, pp. 213–215.

BRUNT, D., 1944, *Physical and Dynamical Meteorology*, 2nd ed., pp. 48, 87. Cambridge University Press.

DEACON, E. L., 1953, Vertical profiles of mean wind in the surface layers of the atmosphere. *Geo-*

*physical Mem.*, **91**. Air Ministry, Meteorol. Office, London.

EMMONS, G. and MONTGOMMERY, R. B., 1947, Note on the physics of fog formation. *J. Meteor.*, **4**, p. 206.

FLEAGLE, R. G., 1953, A theory of fog formation. *J. Marine Res.*, **12**, pp. 43–50.

FLEAGLE, R. G., 1956, The temperature distribution near a cold surface. *J. Meteor.*, **13**, pp. 160–165.

FLEAGLE, R. G., PARROT, W. H. and BARAD, M. L., 1952, Theory and effects of vertical temperature distribution in turbid air. *J. Meteor.*, **9**, pp. 53–60.

HANN, J., 1874, Über den Einfluss des Regens auf den Barometerstand und über die Entstehung der Niederschläge im Allgemeinen. *Met. Zeitschr.*, **9**, pp. 289–296. Österreichische Gesellschaft für Meteorologie.

IMAHORI, K., 1953, On the vanishing mechanism of advection fog and the role of turbulence. *Studies on Fog, Institute of Low Temperature Science*, pp. 35–67. Hokkaido University, Sapporo.

KRAUS, H., 1958, Untersuchungen über den nächtlichen Energiehaushalt in der bodennahen Luftschicht bei der Bildung von Strahlungsnebeln. *Berichte des Deutschen Wetterdienstes*, **48**.

KUROIWA, D., 1953, The turbulent diffusion of fog water near the ground and the fog-preventing effect of an artificial model forest. *Studies on Fog, Institute of Low Temperature Science*, pp. 279–302. Hokkaido University, Sapporo.

KUROIWA, D. and KINOSITA, S., 1953, A balloon fog meter and the vertical distribution of liquid water contents in lower atmosphere. *Studies on Fog, Institute of Low Temperature Science*, pp. 187–204. Hokkaido University, Sapporo.

LILJEQUIST, G. H., 1957, Energy exchange of an antarctic snow field. *Norwegian–British–Swedish Antarctic Expedition, 1949–52. Scientific Results*, **2**, pp. 270–275. Norsk Polarinstitutt, Oslo.

MORALES, C., 1958, Synoptic and mesoaerological study of radiation fog. *Arch. Meteor., Geophys. u. Bioklimat. Ser. A*, **10**, pp. 387–409.

NYBERG, A., 1949, On liquid water content in fogs and clouds. *Swedish Meteorological and Hydrological Institute, Communications Ser. B*, **6**.

PERNTER, J. M., 1882, Berechnung der Niederschlagsmengen bei Mischung feuchter Luftmassen von verschiedener Temperatur. *Met. Zeitschr.*, **17**, pp. 421–426. Österreichische Gesellschaft für Meteorologie.

RIDER, N. E. and ROBINSON, G. D., 1951, A study of the transfer of heat and water vapour above a surface of short grass. *Quart. J. R. Met. Soc.*, **77**, pp. 375–401.

ROBINSON, G. D., 1950, Notes on the measurement and estimation of atmospheric radiation. *Quart. J. R. Met. Soc.*, **76**, pp. 37–51.

SUTCLIFF, R. C., 1948, The physics of fog formation. *J. Meteor.*, **5**, p. 118.

SUTTON, O. G., 1953, *Micrometeorology*, p. 314. McGraw-Hill Book Company, New York.

SVERDRUP, H., 1945, *Oceanography for Meteorologists*, p. 64. George Allen & Unwin Ltd., London.

SWINBANK, W. C., 1955, An experimental study of eddy transports in the lower atmosphere. *Technical Paper*, **2**. C.S.I.R.O. Div. Meteorological Physics, Melbourne.

TAYLOR, G. I., 1917, The formation of fog and mist. *Quart. J. R. Met. Soc.*, **43**, pp. 241–268.

TIMOFEEV, M. P., 1955, K teorii advektivnykh tumanov (Theory of advection fogs). *Akademiia Nauk SSSR, Izvestiia Ser. Geofiz.*, **6**, pp. 514–520.

URFER, A., 1956, Sur les changements du gradient verticale de température dans le brouillard de rayonnement. *Geof. Pura e applicata*, **34**, pp. 231–245.

URFER, A., 1957, Brouillards de rayonnement et gradient vertical de température. *La Météorologie Ser. 4*, **45–46**, pp. 101–107.

WEBER, H., 1912, *Die partiellen Differential-Gleichungen der Matematischen Physik*, 5th ed., vol. 2, pp. 90–121. Friedr. Vieweg & Sohn, Brunswick.

WETTSTEIN, H., 1869, Die Beziehung der Elektrizität zum Gewitter. *Vierteljahrsschrift d. Naturf. Ges. Zürich*, **14**, pp. 60–103.